ANALYSIS OF SEAWIFS OCEAN COLOR ALGORITHMS FOR LAKE ERIE

A Thesis

Presented in Partial Fulfillment of the Requirements for

The Degree of Master of Science in the

Graduate School of The Ohio State University

By

Christopher Everett Wells, B.S.

The Ohio State University

2005

Master's Examination Committee

Dr. Carolyn J. Merry, Advisor

Dr. Diane Foster

Dr. Timothy Granata

Approved by

Carolyn J. Merry

Advisor
Graduate Program in Civil Engineering

ABSTRACT

Cyanobacteria, or blue-green algae, present an increasing threat to the health of many people living in the Lake Erie Basin. Some of these blue-green algae can have a significant and adverse effect on water quality. Blue-green algae can also provide an increase in disease-pathway availability, as well as an increase in toxic chemicals, such as microcystin, in water supplies. Concentrations of cyanobacteria can be detected by measuring chlorophyll-a in their cellular structure, although in situ detection of these toxic cyanobacteria on the scale necessary for water supply treatment and determination of beach closings is not generally economically feasible. Algorithms for chlorophyll-a concentration detection using imagery from the Sea-viewing Wide Field-of-View Sensor (SeaWiFS) have had successes in the ocean, but have not yet been applied extensively to fresh water, and use of these algorithms in the Great Lakes has been limited.

The main objective of this research is to examine how well five ocean color algorithms perform in predicting chlorophyll-a concentrations in fresh water. Values for the normalized water leaving radiance and the remotely sensed reflectance were determined for the wavelengths of 443, 490, 510, and 555 μm using the SeaWiFS Data Analysis System (SeaDAS). The normalized water leaving radiances and remotely sensed reflectances from SeaWiFS were used to approximate chlorophyll-a concentrations. Five ocean color algorithms, CalCOFI-3, Aiken-P, Aiken-C, OC4, and OC4v4, were evaluated. The nearest neighbor, spatial averaging, bilinear averaging, and

inverse distance weighted (IDW) methods were used for estimating a SeaWiFS data value of chlorophyll to compare with measured ground truth data of chlorophyll-a concentration.

IDW produced less scatter in the prediction of chlorophyll-a concentrations for the in situ data examined, resulting in an average R^2 value of 0.35. A similarity of three of these algorithms (OC4v4, OC4, and CalCOFI-3) is by use of the 510:555 band ratio, which at concentrations greater than 3 μg/L, showed the best correlated index of chlorophyll-a. For the CalCOFI-3 algorithm, the 510:555 ratio is weighted less than the 490:555 ratio. The OC4 ocean color algorithm uses the 510:555 ratio only when it is the maximum of three band ratios – 443:555, 490:555, and 510:555. The OC4v4 algorithm is the successor to the OC4 algorithm and was developed using other in situ data – specifically data where the concentrations were similar to those observed for this study area of Lake Erie. Twenty-six of the 37 data points for the study site used in this analysis were found to have concentrations greater than 3 μg/L. The OC4v4 ocean color algorithm was found to most accurately predict observed chlorophyll-a concentration when compared to in situ data (R^2=0.38).

In conclusion, use of the OC4v4 algorithm and the IDW sampling method is best suited for determination of chlorophyll concentrations in Lake Erie using SeaWiFS imagery.

To my mother,
Watch over and keep me, guide me, and protect me.

ACKNOWLEDGEMENTS

I would like to thank my committee for taking the time to assist me in completing this project. These include:

Dr. Merry for her help, support, and guidance throughout my undergraduate and graduate career. Without her, this never would have been possible.

Dr. Foster for making differential equations seem easy, and for always making me think harder than I wanted to.

Dr. Granata for showing me Engineering is not only math, but science and people as well.

Dr. David Culver and Joseph D Conroy (Department of Evolution, Ecology, and Organismal Biology, The Ohio State University) for providing the in situ data collected under the grant sponsored by Federal Aid in Sport Fish Management (F-69-P), administered jointly by the U.S. Fish and Wildlife Service and the Ohio Division of Wildlife.

My loving wife Debi, for all her support these past years.

Raghu Mupparthy for all his technical support.

The SeaWiFS Project (Code 970.2) and the NASA Goddard Earth Sciences Data and Information Services Center/Distributed Active Archive Center (Code 902) at the NASA Goddard Space Flight Center, Greenbelt, MD 20771, for the production and distribution of these data, respectively. May our ocean-color community survive the coming century, and may we keep reaching for the sky.

OhioView Consortium for helping to fund my research.

And last, but not least, all the members of the coastal and remote sensing lab for lending technical support throughout this project.

VITA

August 17, 1979.................................... Born – Huntington, West Virginia

2003... B.S. Civil/Environmental Engineering, The Ohio State University

2003-present... Graduate Teaching and Research Associate, The Ohio State University

FIELDS OF STUDY

Major Field: Civil/Environmental Engineering

TABLE OF CONTENTS

LIST OF TABLES

LIST OF FIGURES

CHAPTER 1

INTRODUCTION

The Great Lakes contain 84% of North America's supply of fresh surface water and 21% of the world's supply of fresh water. With increased development around and demand of water from the Great Lakes, and Lake Erie in particular, the quality of the lake water is becoming a concern. One of the concerns is the increasingly frequent blue-green algal blooms in the Great Lakes. These blooms have the potential not only to cause economic and social impacts, but are also a human health concern. Blue-green algal species, such as *Microcystis*, can release toxins into the water in concentrations that can cause liver cancer and gastro-enteritis, among other complications.

The causes of these algal blooms are not completely understood at this time. One possible contribution could result from introduction of non-indigenous species, such as *Dreissena polymorpha* (zebra mussels) and *Dreissena bugensis* (quagga mussels). These invasive species are known to be a route of transfer and biomagnification of microcystin (a toxin released by some strains of *Microcystis*) through their feces and pseudofeces (Culver et al., 1999). Other potential contributing factors could result from increased light penetration due to decreases in lake water levels, from increased production due to increases in nutrient loading from non-indigenous species, both from the introduction of non-indigenous species or changes to the ecosystem via anthropogenic influx. If the distribution of these algal blooms could be predicted and mapped accurately, more information could be gathered to determine their causes.

Monitoring of algal blooms is an expensive and time-consuming effort. In situ water samples must be collected and then analyzed by visible spectrophotometry in the laboratory. Accurate models have been shown to relate chlorophyll-a concentration to blue-green algal concentrations within a lake environment, allowing the spatial distribution of the chlorophyll to be mapped. The Sea-viewing Wide Field-of-view Sensor (SeaWiFS) is ideal for this purpose, because of its high radiometric resolution and its spectral band widths that have been specifically designed to be sensitive to changes in ocean color.

Several models have been developed using SeaWiFS imagery for coastal and open ocean areas. These models range from power functions of simple band ratios in the case of the OC1a algorithm to modified cubic polynomials of maximum band ratios, as in the case of the OC4 algorithm. All of the current algorithms were developed for open ocean conditions – classified as Case I waters, since living algal cells, associated debris, dissolved organic matter and gelbstoffe solely influence the optical properties by absorption and scattering (Gordon and Morel, 1983). However, Lake Erie is typically classified as a Case II water. This is because its optical properties are determined by resuspended sediments, terrigenous particles, dissolved organic matter from land drainage and anthropogenic influx, as well as the constituents that influence Case I waters. Only one of these extra four components is needed to define a Case II water. Lake Erie has all four components. Gordon and Morel (1983) suggested that improved accuracy of ocean color models for Case II waters might be achievable on a local basis using adapted algorithms. This is because of the relationships that exist between the additional constituents and the water reflectance properties. Since the resuspended sediments, terrigenous particles, dissolved organic matter from land drainage, and anthropogenic influx can all be characterized as localized phenomena, it is possible that these factors can be studied in more detail and taken into account for modifying developed ocean color algorithms.

Mupparthy and Merry (2004) evaluated 17 chlorophyll prediction models for Lake Erie that were initially developed for Case I waters using SeaWiFS data. The models were tested against a limited data set of in situ observations of chlorophyll-a and downwelling and upwelling radiance profiles taken at four locations in Lake Erie. They identified four out of the 17 models that showed promise. The goal of this research is to test these four models, and one additional model for historical purposes, against ground truth data acquired in western and central Lake Erie during two summers to determine which model provided the best prediction of chlorophyll-a concentration.

CHAPTER 2

BACKGROUND

Understanding the water body characteristics of Lake Erie is imperative for interpreting the extent and distribution of chlorophyll-a concentrations. Lake Erie provides a dynamic area for the study of chlorophyll distributions and algal bloom causes, with its diverse bathymetry, biology, and history. This chapter provides a discussion of the study area, a review of blue-green algae species present in Lake Erie, and the remote sensing data sets that are available for mapping water quality parameters.

2.1: Study Area Description

Lake Erie is the oldest of the five Great Lakes (Figure 2.1). Formed after the glacial retreat approximately 9,000 years ago, Lake Erie is also the shallowest of the Great Lakes with an average depth of 19 m. Lake Erie is the smallest in terms of volume (484 km^3) and is the second smallest lake in terms of surface area (25,700 km^2) (Environment Canada and USEPA, 1995). Lake Erie has survived three glacial expansions, numerous invasive species introductions, such as *Dreissena polymorpha* (zebra mussels), and nutrient loading from a variety of agricultural activities. Despite these threats, Lake Erie continues to provide both recreational and commercial fishing, and shipping. In addition to this, three major metropolitan areas (Cleveland, Ohio, Toledo, Ohio, and Buffalo, New York) use Lake Erie as the source for the majority of their drinking water.

In the 1950s and 60s, the Cuyahoga River in Cleveland, Ohio, caught fire numerous times from oil and debris that had been dumped into the river. The lack of environmental standards and monitoring had resulted in the lake being a repository for municipal, industrial and commercial waste, as well as nutrients– especially phosphorous and nitrogen from non-point agricultural sources. Studies showed that the lake was overloaded with these nutrients, so much so that it was declared "dead" in the late 1960s (Leahy, 2003).

Environmental standards were implemented starting in the 1970s, nutrient loading was reduced, and over time, the lake was thought to be improving. During the 1970s and 80s phosphorous levels were observed to be decreasing. While still suffering from eutrophication, a condition in which biological productivity is high and the water is extremely rich in nutrients, the ecological health of Lake Erie was rebounding. One indicator of water quality improvements in recent years include the resurgence of *Hexagenia* (mayflies) (Environment Canada and USEPA, 2003). However, over the past few years *Dreissena polymorpha* (zebra mussels) and *Dreissena bugensis* (quagga mussels), as well as *Lythrum salicaria* (purple loosestrife), *Phragmites australis*, and *Neogobius melanostomus* (round gobies), have been introduced. With the introduction of these non-indigenous species, phosphorous levels have been observed to be increasing again. Algal blooms are now large enough where they can be easily seen on satellite images. One of the species that shows an increase in annual blooms is *Microcystis aeruginosa*.

There are 12 different species of *Microcystis* found in eutrophic lakes (Park and Watanabe, 1996). While in their dormant stage, these coccolithic cyanobacteria form cysts that are denser than water. In approximately June or July, they "bloom" and rise to the surface, continuing growth typically throughout September, when they return to their dormant stage. The cyanobacteria typically grow in eutrophic or hypereutropic lakes (Park and Watanabe, 1996), making Lake Erie a perfect environment. Though present in the lake during the 50s and 60s, few people thought to give the cyanobacteria credit for the massive fish kills, since xenobiotics – manmade compounds with chemical structures foreign to a given organism – were thought to be the culprit (NOAA Sea Grant, 1995). However, today more and more scientists are recognizing how toxic these single celled organisms can be.

While *Microcystis* is active, toxins known as microcystins are produced as a product of photosynthesis. In nature, blooms containing various species of *Microcystis* have been found to produce up to 23 different microcystins (Sivonen and Jones, 1999). *Microcystis aeruginosa*, one of the species tentatively identified as being present in Lake Erie, produces Microcystin-LR, a highly toxic hepatotoxin. Hepatotoxins are substances capable of causing damage to the liver. While the primary target in mammals is the liver, microcystins have also been shown to target the kidney, lungs, and intestines. In Qidong county in the People's Republic of China, an epidemiological study showed that a high incidence of primary liver cancer was strongly correlated to microcystin contamination of the water supply (Fujiki et al., 1996). Studies on mice have shown that ingestion of microcystins induce neoplastic liver nodules (Kuiper-Goodman et al., 1999). In Harare, Zimbabwe, human gastro-enteritis was linked to a water source where an annual bloom of *Microcystis* occurred (Zilberg, 1966). A study on Lake Erie during the summers of 1995 and 1996 showed that the concentrations of microcystins are ~5 x 10^{-10} times below the human liver toxicity threshold (Culver et al., 1999). The earlier studies by Fujiki (1996) and Zilberg (1966) demonstrate a need for monitoring and controlling the *Microcystis* species. Even if Lake Erie shows such small concentrations, the potential exists for increases in *Microcystis* levels in Lake Erie that could prove to be of concern.

2.2: Available Remote Sensing Data Sets for Use in Water Quality

There exists a historical basis for mapping ocean properties utilizing satellite imagery. In 1978, NASA launched the NIMBUS-7 environmental satellite. One of the sensors on this satellite was the Coastal Zone Color Scanner (CZCS) sensor that focused on water quality. Launched as a proof-of-concept mission, this scanner allowed scientists "their first opportunity to observe the [variability] of global biological productivity" (Acker, 1994). Six spectral bands were included on the CZCS sensor (Table 2.1).

Channel	Wavelength (μm)	Principal Parameter
1	0.43-0.45	Chlorophyll absorption
2	0.51-0.53	Chlorophyll absorption
3	0.54-0.56	Gelbstoffe (yellow substance)
4	0.66-0.68	Chlorophyll concentration
5	0.70-0.80	Surface vegetation
6	10.50-12.50	Surface temperature

Table 2.1: Spectral Bands of the Coastal Zone Color Scanner (Lillesand et al., 2004)

The NIMBUS Experiment Team (NET) was formed as a group of optical physicists and biological oceanographers that wanted to validate the radiometric measurements observed by the CZCS, as well as to relate the satellite data to standardized measurements of biological productivity and optical seawater clarity. Using the NET data set, consisting of oceanographic stations in the Atlantic and Pacific Oceans, the Gulf of Mexico and the Gulf of California, the team developed atmospheric correction methods, as well as pigment algorithms. Virtually all of these algorithms utilize band ratios to quantify the chlorophyll concentrations, phaeopigment concentrations, and total pigment concentrations. The results of these CZCS experiments were used in recommending the spectral bands for the next generation satellite sensor, SeaWiFS, that was focused on water properties.

The SeaStar satellite was launched in 1997 as part of NASA's Earth Science Enterprise (ESE) mission (Chandler, 1998). The mission of the ESE is "to develop a scientific understanding of the Earth system and its response to natural and human-induced changes to enable improved prediction of climate, weather, and natural hazards for present and future generations" (NASA Earth Observatory, 2002). Under an arrangement known as a "data buy," "NASA contracted with Orbital Sciences Corporation (OSC) to build, launch and operate SeaWiFS on the OSC OrbView-2 satellite (which was later renamed to SeaStar) to meet NASA's science requirement for ocean monitoring data" (Lillesand et al., 2004). This was one of the first commercial satellites to provide daily images of the earth. NASA purchased the SeaWiFS data and offered it free of charge to authorized SeaWiFS research users until 23 December 2004, when the existing data buy agreement expired. Data acquired after that date are available, but must be purchased directly from OSC. As of February 14, 2005, the NASA Stennis Space Center Acquisition Management Office announced that it planned to issue a contract to OSC for SeaWiFS imagery, which could potentially extend the period of free access to SeaWiFS data for authorized SeaWiFS researchers (NASA Procurement Office, 2005).

The SeaStar satellite travels in a sun-synchronous orbit at an altitude of 705 km with an inclination angle of 98.2°. The satellite crosses the equator at noon daily on its descending node. SeaWiFS is an across-track or "whiskbroom" scanner. The orbital path provides the north/south movement, while the rotating scanning telescope coupled with the half-angle scan mirror arrangement provides the east-west movement. The scan mirror goes through six revolutions per second (Hooker et al., 1992). The instantaneous field of view (IFOV) of SeaWiFS results in a spatial resolution of 1.13 km for Local Area Coverage (LAC) images at nadir, which are then resampled for the 4.5 km spatial resolution Global Area Coverage (GAC) images. The swath width is 2,801 km (LAC) and 1,502 km (GAC). The geometric error in location of a ground resolution cell can be ±0.5 pixel.

SeaWiFS images are received by OSC HRPT stations, which create level 1a images. "Level 1a image data are raw, and all spacecraft and instrument telemetry are retained in raw form as in the Level 0 data. In addition, geolocation data, instrument telemetry and selected spacecraft telemetry are converted and appended" (SeaDAS Development Group, 2002). Users can download the level 1a images from the Distributed Active Archive Centers (DAACs) and process them with the SeaWiFS Data Analysis System (SeaDAS) to generate their own level 1b (sensor calibration applied), level 2 (atmospherically corrected, sensor calibration and bio-optical algorithms applied), or level 3 (spatially projected level 2) image products. Functions in SeaDAS allow queries of latitude and longitude or pixel/line coordinates for use in data extraction. The SeaWiFS sensor has eight spectral bands (Table 2.2).

Band	Wavelength (nm)	Midpoint of Spectral Band
1	402-422	412
2	433-453	443
3	480-500	490
4	500-520	510
5	545-565	555
6	660-680	670
7	745-785	765
8	845-885	865

Table 2.2: Spectral Bands of the Sea-viewing Wide Field-of-view Sensor (Lillesand et al., 2004)

The SeaWiFS sensor is unique in that the spectral bands are sensitive to fluctuations in ocean color that are due to pigment changes caused by variations of phytoplankton, changes in suspended matter, and changes in organic carbon, among others. Other satellite data, such as Landsat Thematic Mapper and the Advanced Very High Resolution Radiometer (AVHRR), have been used to monitor changes in ocean color, although these sensors were not specifically designed for deriving water properties.

Stumpf (1987) utilized AVHRR data to study sediment and chlorophyll in the turbid coastal water of the Chesapeake Bay. The AVHRR is an 11-bit sensor on the NOAA satellites, with twice daily coverage and a spatial resolution of 1.1 km at nadir. However, its spectral resolution is significantly less than SeaWiFS (Table 2.3) with wider bandwidths and a reduced number of spectral bands.

Band	Wavelength (μm)
1	0.58-0.68
2	0.72-1.10
3	3.55-3.93
4	10.3-11.30
5	11.5-12.50

Table 2.3: Spectral Bands of the AVHRR sensor (Lillesand et al., 2004)

Stumpf (1987) found that measurement of sediment concentration may be as accurate as ±30%, and estimates of chlorophyll may be estimated to within 60% at concentrations greater than 10 μg/L. At concentrations below 10 μg/L, the error is ±5 μg/L. The greatest error in estimating chlorophyll concentrations was attributed to the uniform atmospheric correction being applied to the image data. The atmospheric correction scheme is sensitive to heterogeneities in the atmosphere or incorrect estimates of the atmosphere resulting in a scene bias. Corrections made to SeaWiFS data would later attempt to take this problem into account by utilizing localized meteorological data when performing the atmospheric correction.

In 1984, the Thematic Mapper (TM) sensor was launched onboard the Landsat-5 satellite. This sensor features much higher spatial resolutions (30 m for bands 1-5 and 7, 120 m for band 6), however, the temporal resolution is much less than SeaWiFS – 16 days rather than 1 day. The radiometric resolution is also lower for the TM sensor, 8-bit (256) as opposed to 10-bit (1024) data. The TM sensor spectral band widths are wider than SeaWiFS (Table 2.4).

Band	Wavelength (μm)
1	0.45-0.52
2	0.52-0.60
3	0.63-0.69
4	0.76-0.90
5	1.55-1.75
6	10.4-12.5
7	2.08-2.35

Table 2.4: Spectral Bands of the Landsat-5 TM sensor (Lillesand et al., 2004)

Budd et al. (2001) utilized Landsat TM imagery in conjunction with data from the AVHRR to observe *Microcystis* blooms in western Lake Erie. The study found that it was impossible to separate chlorophyll and sediment using the AVHRR data. However, with only seston (a measure of particulate matter, such as plankton, organic detritus and inorganic particles) data, and no shipboard sampling data collected during the blooms, chlorophyll concentrations were not directly estimated utilizing the AVHRR data. According to Budd et al. (2001), Landsat TM's ability to "resolve fine-scale spatial patterns allows for separation of the sediment and pigment signals". Budd et al. (2001) states that "TM's four visible channels are ample for estimating chlorophyll concentrations, as well as sediment". Landsat TM images were used by Budd et al. (2001) to estimate the chlorophyll concentrations, but only in a qualitative sense to illustrate the areal extent of the blooms. A shortcoming of Budd et al. (2001) is that no clear method for estimating chlorophyll concentrations, nor sediment concentrations, was given.

SeaWiFS has the same radiometric resolution as the AVHRR sensor (10-bit), and is comparable in temporal and spatial resolution. Where SeaWiFS truly demonstrates its usefulness as an ocean color sensor following the CZCS, TM, and the AVHRR for ocean color applications is in the spectral resolution, having eight bands between 400-900 nm (Figure 2.2). The CZCS only has five bands in this range, lacking any between 450-500 nm, which were included on SeaWiFS to monitor gelbstoff and sediments (Hooker, 1992). Thematic Mapper only has four bands between 400-900 nm, with much wider band widths than those for SeaWiFS. SeaWiFS bands 3 and 4 were selected by the design team to focus on ocean color due to the properties of chlorophyll in these regions. These two spectral bands are not separate on the Landsat TM sensor. Cyanobacteria have a distinct absorption from 540 nm to 560 nm (Bisset et al., 2001). SeaWiFS band 5 (centered on 555 nm) is primarily designed to monitor this region of the spectrum to facilitate detection of blue-green algae. Since the Landsat TM band widths are much wider (0.45-0.52 and 0.52-0.60 μm), the TM sensor cannot detect this absorption band.

Figure 2.1: Location of Lake Erie in the northeastern United States (source: Shape file from ESRI ArcGIS software).

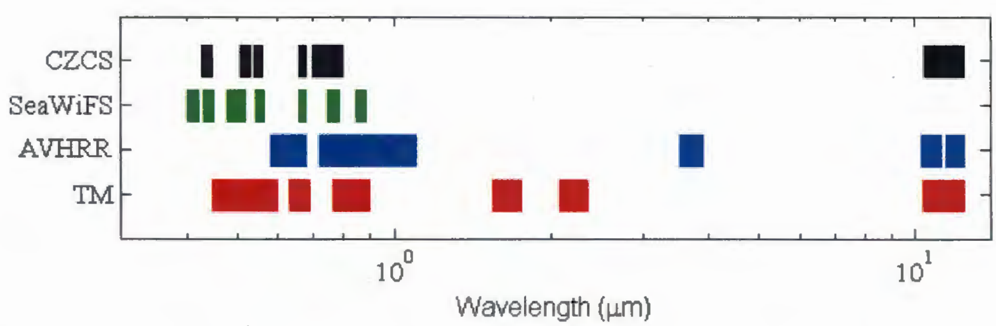

Figure 2.2: Spectral band coverage of the CZCS, SeaWiFS, AVHRR, and Thematic Mapper satellite sensors.

CHAPTER 3

LITERATURE REVIEW

The previous chapter examined different approaches to satellite observation of ocean color. This chapter will provide an examination of algorithms designed for chlorophyll monitoring utilizing SeaWiFS imagery, as well as different sampling methodologies used to extract representative data from SeaWiFS images.

3.1: Description of ocean color algorithms

Aiken et al. (1995) examined the NET and Bio-optical Synthetic Model (BSM) data to generate a band ratio algorithm for the SeaWiFS sensor data that would offer continuity with CZCS measurements. One algorithm was required for chlorophyll and pigment concentrations and another algorithm was needed for strictly chlorophyll concentrations. They settled on equations that best fit the data for seawater conditions using an analytical form of the equations and empirical coefficients. Both of the equations were based on the ratio of the water leaving radiances (L_{WN}) at 490 and 555 nm. The water leaving radiance equation, L_{WN}, is:

$$L_{WN} = F_0\left[\frac{(1-\rho)(1-\tilde{\rho})R}{n^2(1-rR)Q}\right] \tag{3.1}$$

where F_0 is the extraterrestrial irradiance, n is the refractive index of seawater, R is the irradiance reflectance, ρ is the Fresnel reflectance at normal incidence, $\tilde{\rho}$ is the Fresnel reflectance for sun and sky irradiance, r is the air-water reflectance for diffuse irradiance, and Q is the ratio of upwelling irradiance to radiance.

Aiken et al. (1995) states that the main determinant of the radiance ratio, L_{WN}, is the irradiance reflectance, R, expressed as:

$$R(\lambda) = G(\mu_0, \lambda)\left[\frac{b_b(\lambda)}{a(\lambda)}\right] \tag{3.2}$$

where $G(\mu_0, \lambda)$ represents the effect of the downwelling light field, $b_b(\lambda)$ is the backscatter coefficient; and $a(\lambda)$ is the absorption coefficient. They combined the ratios of the air-sea interface effects, the effects of the light field, and the relative spectral variation of Q to obtain the constant g, which they assumed to be unity. The radiance ratio R_{ij} becomes:

$$R_{ij} = \frac{L_{WN}(i)}{L_{WN}(j)} = \frac{F_0(\lambda_i)\left[\dfrac{(1-\rho)(1-\tilde{\rho})G(\mu_0,\lambda)\left[\dfrac{b_b(\lambda_i)}{a(\lambda_i)}\right]}{n^2(1-rR)Q}\right]}{F_0(\lambda_j)\left[\dfrac{(1-\rho)(1-\tilde{\rho})G(\mu_0,\lambda)\left[\dfrac{b_b(\lambda_j)}{a(\lambda_j)}\right]}{n^2(1-rR)Q}\right]} = \frac{a(\lambda_j)b_b(\lambda_i)F_0(\lambda_i)}{a(\lambda_i)b_b(\lambda_j)F_0(\lambda_j)} \tag{3.3}$$

After analyzing the NET and BSM data, the best chlorophyll (C) algorithm (Aiken-C) defined by Aiken et al. (1995) was determined to be:

$$\begin{aligned} C &= e^{0.464-1.989\log(R)} \quad \text{if } C > 2.0\frac{\mu g}{L} \\ C &= \frac{(R-5.29)}{(0.719-4.23R)} \quad \text{if C} < 2.0\frac{\mu g}{L} \end{aligned} \tag{3.4}$$

The best pigment (P) and chlorophyll concentration algorithm (Aiken-P) defined by Aiken et al. (1995) was determined to be:

$$
\begin{aligned}
C &= e^{0.696-2.085\log(R)} = [C+P] \text{ if } [C+P] > 2.0\frac{\mu g}{L} \\
C &= \frac{(R-5.29)}{(0.592-3.48R)} = [C+P] \text{ if } [C+P] < 2.0\frac{\mu g}{L}
\end{aligned}
\qquad (3.5)
$$

In 1998, the California Cooperative Oceanic Fisheries Investigations (CalCOFI) team analyzed data from the Southern California Bight region (Mitchell and Kahru, 1998). They explored ratios of remotely sensed radiance (R_{rs}), as well as the water leaving radiance (L_{WN}), and determined that algorithms utilizing band ratios of L_{WN} resulted in slightly higher r^2 values and lower root-mean-squared (RMS) error. One of the equations developed by Mitchell and Kahru (1998) was a three-band ratio algorithm (CalCOFI-3) defined as:

$$
\begin{aligned}
R_1 &= \ln\left(\frac{L_{WN}(490)}{L_{WN}(555)}\right) \\
R_2 &= \ln\left(\frac{L_{WN}(510)}{L_{WN}(555)}\right) \\
C &= e^{1.025-1.622R_1-1.238R_2}
\end{aligned}
\qquad (3.6)
$$

This equation was found to have better results than a similar equation using remotely sensed reflectance (R_{rs}) instead of L_{WN}. The definition of R_{rs} is:

$$
R_{rs} = \frac{L_{WN}}{E_D} \qquad (3.7)
$$

where L_{WN} is the water leaving radiance and E_D is the downwelling irradiance.

Later the same year, O'Reilly et al. (1998) examined the CalCOFI algorithms (using R_{rs} instead of L_{WN}) along with many others, including the Aiken-C and Aiken-P equations. The CalCOFI-3 equation was found to be better suited to the results of the SeaWiFS Bio-optical Algorithm Mini-Workshop (SeaBAM) dataset. Another algorithm, OCTS-C, resulted in a higher r^2 value (0.933) and a non-linear trend. The OCTS-C algorithm is defined as:

$$R = \log\left(\frac{L_{WN}(520) + L_{WN}(565)}{L_{WN}(490)}\right)$$
$$C = 10^{-0.55006 + 3.497R} \tag{3.8}$$

Due to the SeaBAM data set having only R_{rs} values for the in situ data (since all of the data was from before SeaWiFS was launched), the algorithms examined did not consider L_{WN}. Of 12 ocean chlorophyll (OC) algorithms considered by O'Reilly et al. (1998), a modified cubic polynomial maximum 4-band ratio (OC4) was found to fit their data best. The OC-4 algorithm is defined as:

$$R = \max\left\{\begin{matrix} \log 10\left(\dfrac{R_{rs}(443)}{R_{rs}(555)}\right) \\ \log 10\left(\dfrac{R_{rs}(490)}{R_{rs}(555)}\right) \\ \log 10\left(\dfrac{R_{rs}(510)}{R_{rs}(555)}\right) \end{matrix}\right\} \tag{3.9}$$
$$C = 10^{0.4708 - 3.8469R + 4.5338R^2 + -2.4434R^3} - 0.0414$$

O'Reilly et al. (2000) used 2,853 in situ observations from all over the world and further refined the form of the equation which was a modified cubic polynomial to a fourth order polynomial with associated coefficients to create the OC4 version 4 (OC4v4) algorithm, defined as:

$$C = 10^{0.366 - 3.067R + 1.930R^2 + 0.649R^3 - 1.532R^4} \quad (3.10)$$

In a similar study within the region of the western basin of Lake Erie, Mupparthy and Merry (2004) used in situ observations of chlorophyll-a and downwelling radiance profiles and upwelling radiance profiles to evaluate 17 algorithms selected from the ocean color literature. The Aiken-C, Aiken-P, CalCOFI-3, and OC4v4 were the best-suited algorithms for the current atmospheric correction scheme. Consequently, these four algorithms were selected to be evaluated using available in situ data on water quality acquired during 2002 and 2003 in the western and central basins of Lake Erie.

3.2: Mapping a satellite pixel value to correspond to a ground truth sample point

The simplest method of selecting a corresponding satellite pixel to correspond with a ground truth data point is the nearest neighbor method (Figure 3.1). When a point is selected from a satellite image, the value of the pixel (whether it is a digital number, a reflectance value, or some other geophysical value) that is nearest to the coordinates of the given point – the nearest neighbor – is returned. This method does not account for variations over an area, but is commonly used due to its simplicity (Lillesand et al., 2004). In addition, this method preserves the true radiometric characteristics of the image data.

SeaWiFS is an across-track scanner. Inherent in this type of scanner is overlap of the raw data pixels (Figure 3.2). For SeaWiFS at nadir (when the sensor is viewing the ground directly underneath) the spatial resolution is 1.13 km. During preprocessing, the scan line is resampled to 1.1 km pixels. Because of this overlapping nature of adjacent pixels in a scan line, the surrounding pixels have an influence on a pixel's value.

Another way to select a representative pixel value to correlate with a ground sample point is to do spatial averaging (Figure 3.3). A 3x3 matrix of pixels surrounding the location of the in situ data point is extracted and averaged.

Another way to represent a pixel value is to perform a bilinear average (Figure 3.4). Since the point is affected more by the adjacent pixels, only the four neighboring pixels (north, south, east, and west) are taken into account.

These two methods (spatial averaging and bilinear averaging) give equal weight to the nearby pixels. Another option would be to use the Inverse Distance Weighted (IDW) method, specifically the Inverse Distance Squared Weighted Interpolation method (ESRI, 2003). This general formula is:

$$\hat{Z}(s_0) = \sum_{i=1}^{N} \lambda_i Z(s_i) \tag{3.11}$$

where $\hat{Z}(s_0)$ is the value being predicted for location s_0, N is the number of measured sample points surrounding the prediction location that will be used in the prediction (9 in this case), λ_i are the weights for each measured sample point, decreasing with increasing distance, and $Z(s_i)$ is the observed value at each measured sample point. The weights are determined by:

$$\lambda_i = \frac{d_{i0}^{-2}}{\sum_{i=1}^{N} d_{i0}^{-2}} \tag{3.12}$$

where d_{i0} is the distance between the measured sample point and the prediction location.

For this research, the IDW method was used to select a representative satellite pixel value to be used in the ocean color algorithm calculations.

In summary, based upon work by Mupparthy and Merry (2004), five algorithms were investigated and found to be applicable towards Lake Erie. Sampling methodologies were examined for selecting appropriate pixel values to correlate with the in situ data points. The inverse distance weighted interpolation method was used for selecting the satellite data values to compare with the in situ data points. The next chapter will examine the procedures used in data preparation, extraction, processing and analysis.

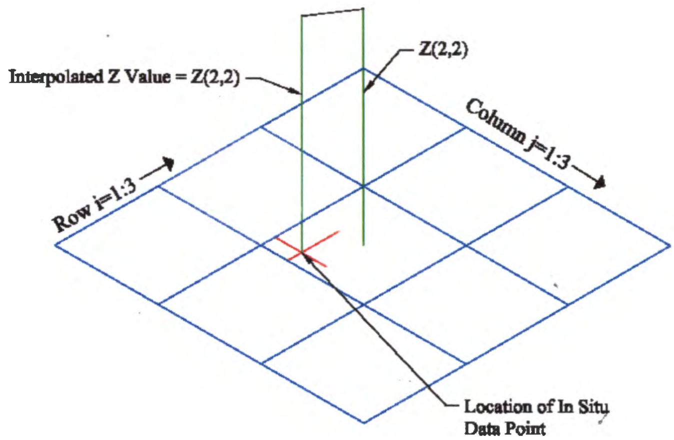

Figure 3.1. Nearest Neighbor Sampling Method

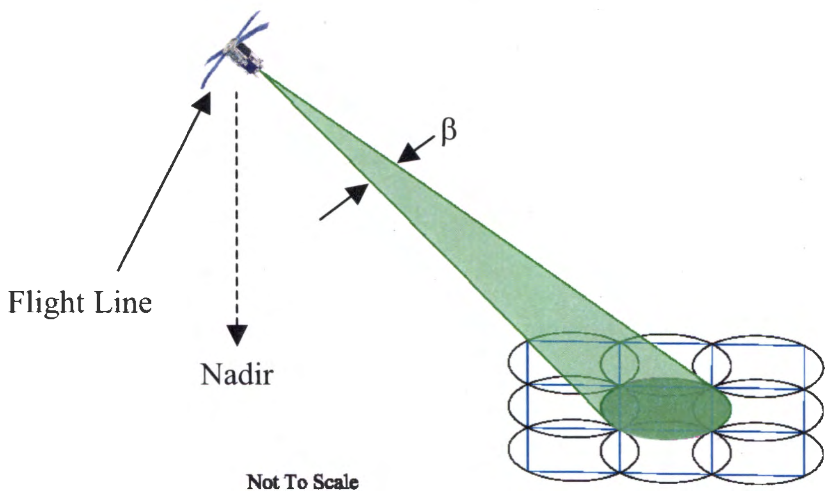

Figure 3.2. Across-track, or whiskbroom, scanner system. The instantaneous field of view (IFOV) is represented as β.

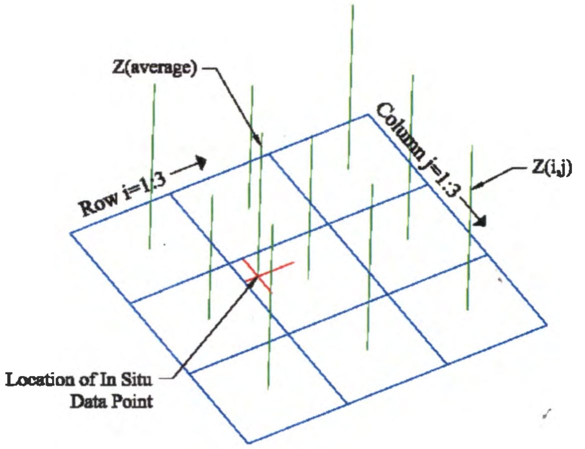

Figure 3.3. Spatial Average Sampling Method

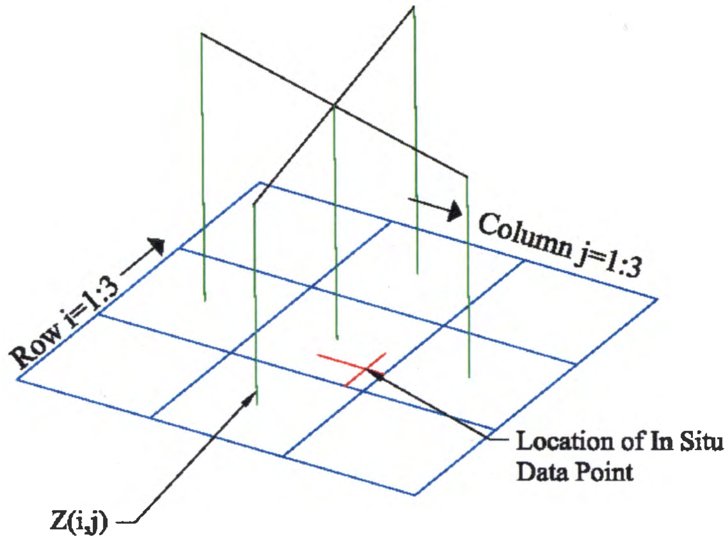

Figure 3.4. Bilinear Average Sampling Method

CHAPTER 4

METHODOLOGY

4.1: In Situ Data Collection and Image Selection

In situ data were provided by J. Conroy (The Ohio State University) and included chlorophyll concentrations at sample site locations in the western and central basins of Lake Erie, for the summer 2002 and 2003. Water samples were obtained by utilizing a 5 cm PVC integrated tube sampler at depths of twice the secchi depth measured. Chlorophyll concentrations were determined by Method 446 by Arar (1997). After receiving the in situ data for the western and central basins of Lake Erie (Table 4.1, Figure 4.1), the coordinates for each sampling point provided were converted from degrees/decimal minutes to decimal degrees (Figures 4.2-4.5). Next, the data set was screened for days that had corresponding cloud-free SeaWiFS images available. These images were downloaded from the Distributed Active Archive Center (DAAC) at the NASA Goddard Space Flight Center (GSFC) in Greenbelt, Maryland (see http://www.daac.gsfc.nasa.gov).

The SeaWiFS images were examined to determine if the sample site was visible. The image data were initially examined to ensure that accurate normalized water-leaving radiance and remotely-sensed reflectance values could be obtained with no level 2 flags (these are pixels that are flagged by the SeaDAS software that could contain high sun glint, land, or cloud shadows). If level 2 flags were found when selecting the image data, the data points were eliminated.

4.2: Satellite Data Preparation

After examining the available data, nine satellite images that corresponded to 37 in situ water samples were found (Appendix A). The corresponding level 1 local area coverage (LAC) image files with 1.1 km spatial resolution were processed using the SeaDAS software. Level 2 images of chlorophyll concentrations using the OC4v4 algorithm – the default algorithm presently available in SeaDAS – such as shown in Figure 4.6, were prepared. Also, the normalized water leaving radiances and remotely sensed reflectance at all wavelength bands were calculated for the nine SeaWiFS images.

Generation of the level 2 images consisted of providing the appropriate meteorological (.met) and ozone (.ozone) data files provided by NASA with the SeaWiFS data, as well as the appropriate sensor calibration files (seawifs_sensor_cal.tbl) to the SeaDAS software. The multiple scattering aerosol model with 7/8 algorithm (Ruddick et al., 2000) and the Siegel Near-InfraRed (NIR) algorithm (Siegel et al., 2000) with up to 10 iterations was used to perform the atmospheric correction on the level 1a images. This is the default atmospheric correction algorithm in SeaDAS.

Next, input text files were prepared with pixel/line values corresponding to the adjacent pixels of the selected sample point. These were then input into the Rline widget in SeaDAS, generating the OC4, and the R_{rs} and L_{wn} values for each SeaWiFS spectral band for the 3x3 pixel matrix for each image. These data were used as input to the four other ocean color algorithms to predict chlorophyll concentrations.

4.3: Bathymetry Data

With the latitudes and longitudes calculated for the SeaWiFS data points, the data sets (in table form) were brought into ArcView. This ArcView table was added to a view as an XY theme and converted to a shape file. Using ArcCatalog, the shapefile was assigned to the World Geographic System Universal Transverse Mercator (1984 Zone 17N) coordinate system to match the coordinate system of a National Oceanographic and Atmospheric Administration (NOAA) bathymetry map. The bathymetry map was created from an x-y-z file obtained from the National Geophysical Data Center (NGDC) at NOAA that was generated from the Great Lakes Bathymetry Grids Database taken at a 3-sec grid size. Secchi depth at each sample point was measured in the dataset provided by J. Conroy.

4.4: Calculations of chlorophyll concentration using the ocean color algorithms

The algorithms (Aiken-P, Aiken-C, OC4, OC4v4 and CalCOFI-3) were used to determine approximate chlorophyll concentration values that corresponded to the locations of the in situ data points. Comparisons between the four sampling methods and the in situ observations were examined. Linear regressions of the predicted and observed chlorophyll concentrations were calculated using the method in Chatterjee and Hadi (1986) in Matlab.

Year	Julian Day	Sample ID	Corrected Chlorophyll-a (μg/L)	Secchi Depth (m)	Depth (m)
2002	222 9 Aug	1	1.104	5.1	-21
		2	0.077984	5.5	-17
		3	1.2723	6.1	-22
		4	0.83705	1.4	-11
	242 30 Aug	1	9.8474	1.1	-6
		2	3.8547	1.5	-9
		3	6.9838	1.2	-10
	249 6 Sep	1	8.6521	0.9	-7
		2	9.4211	1.4	-13
		3	3.6873	4.6	-21
		4	3.5217	3.6	-17
		5	4.045	3.6	-22
		6	3.835	3	-15
2003	174 23 June	1	1.6073	2.5	-21
		2	1.6679	1.8	-17
		3	3.2067	4.2	-22
		4	1.5219	3	-19
		5	2.419	1.7	-11
	176 25 June	1	10.653	2.4	-6
		2	5.4228	1.2	-6
		3	4.8701	4.3	-9
		4	5.4575	2.7	-9
	195 14 July	1	6.0956	1.8	-10
		2	15.144	1.2	-7
		3	2.2561	6	-13
		4	4.1518	1.2	-6
		5	12.225	1.6	-6
		6	9.321	1.5	-9
		7	8.9365	1.8	-9
	210 29 July	1	3.8154	1.2	-6
		2	6.4427	0.9	-6
		3	6.0823	2.4	-9
		4	5.0436	2.1	-7
	253 10 Sep	1	3.1186	4.1	-21
	280 7 Oct	1	2.9904	0.6	-6
		2	6.3546	0.6	-6
		3	2.8462	1.2	-9

Table 4.1: In situ data with derived depth (from J. Conroy, Dept of EEOB, OSU)

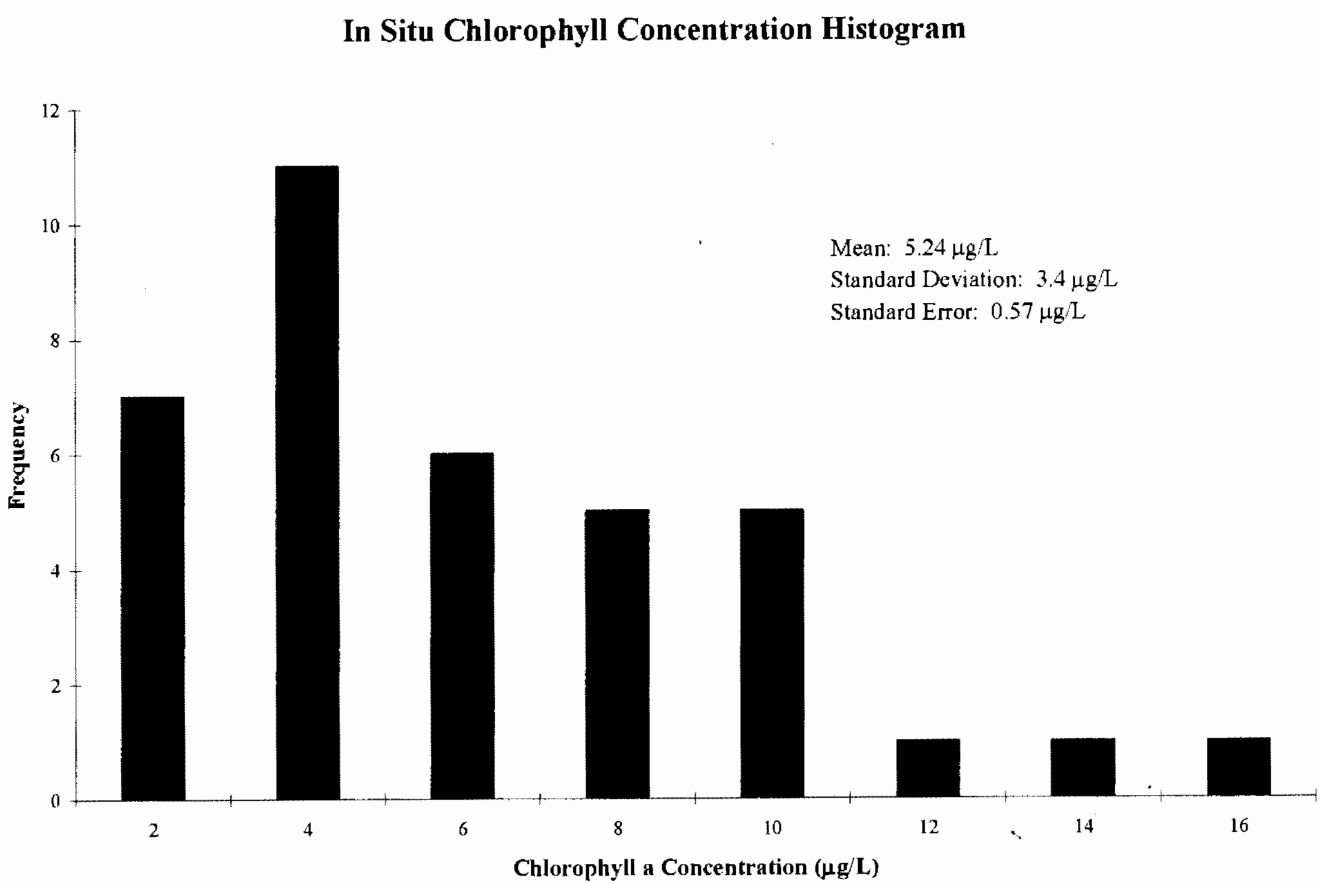

Figure 4.1: Histogram of In Situ Chlorophyll Concentrations.

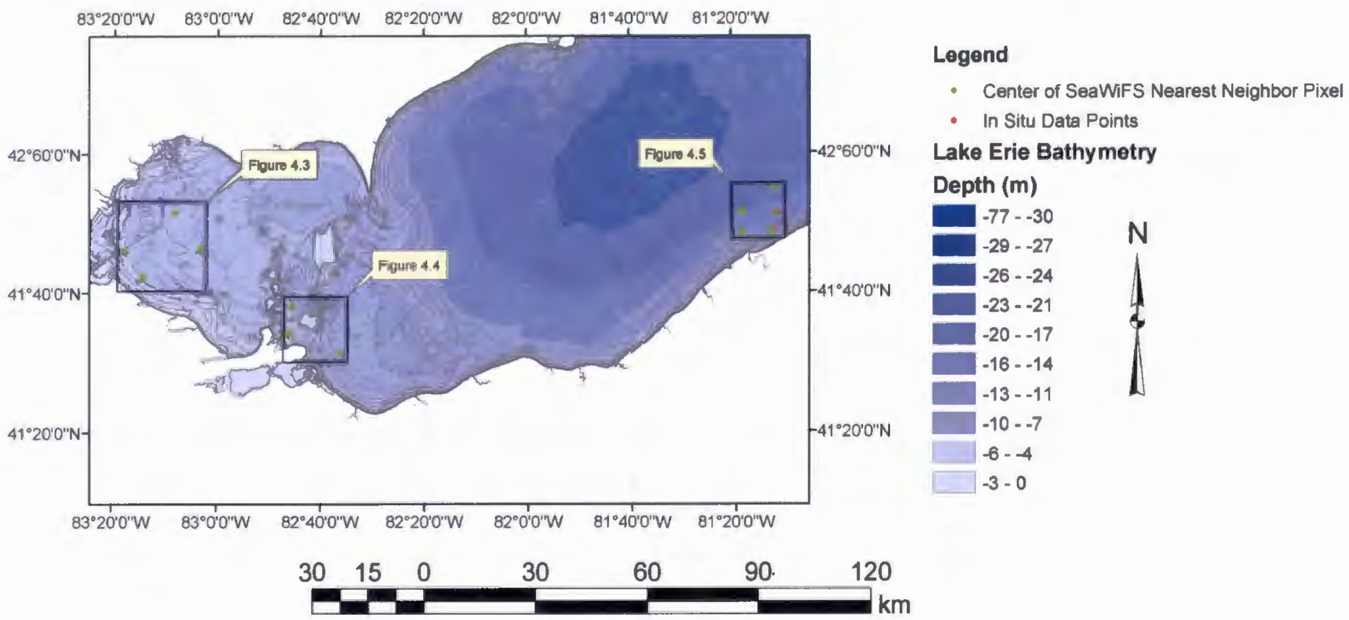

Figure 4.2: Location of the in situ data points and the SeaWiFS image pixel sample locations.

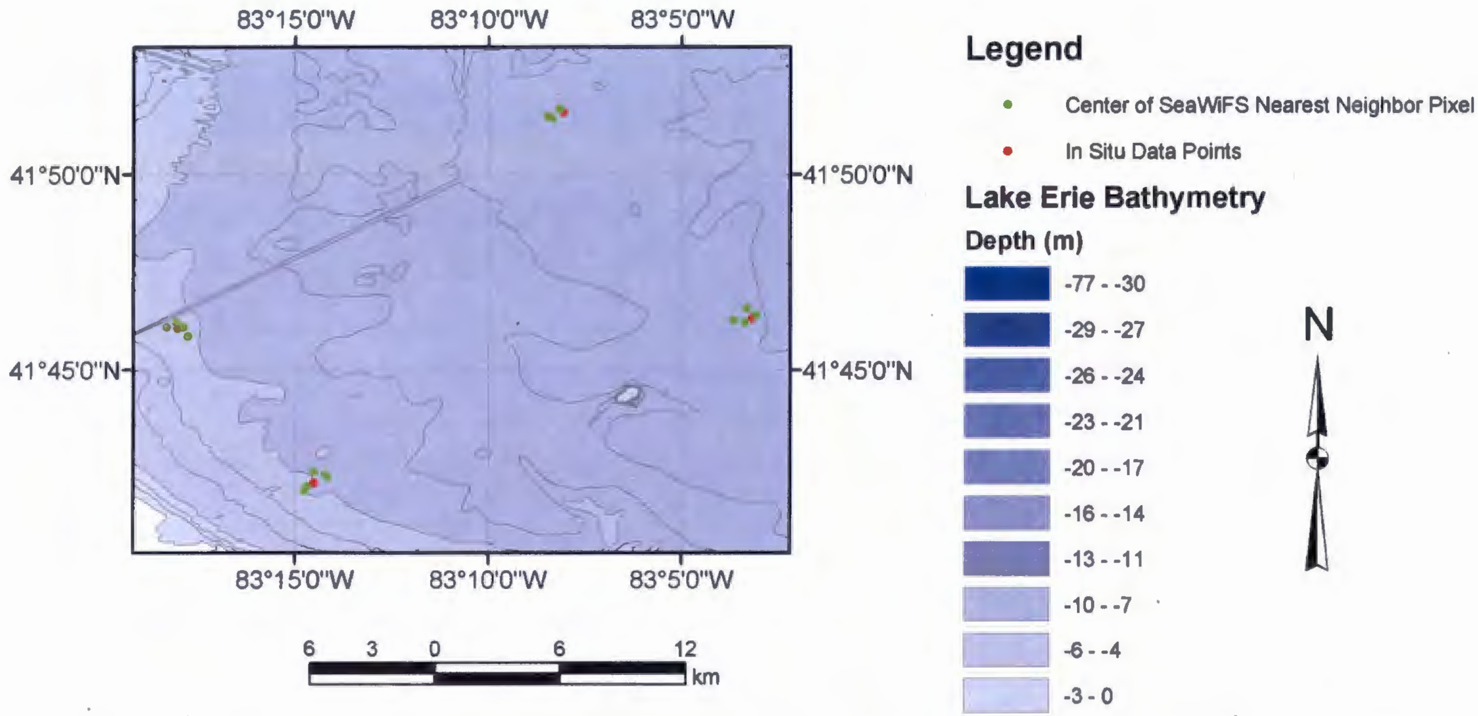

Figure 4.3: Location of the in situ data points and the SeaWiFS image pixel sample locations for the Western Basin of Lake Erie.

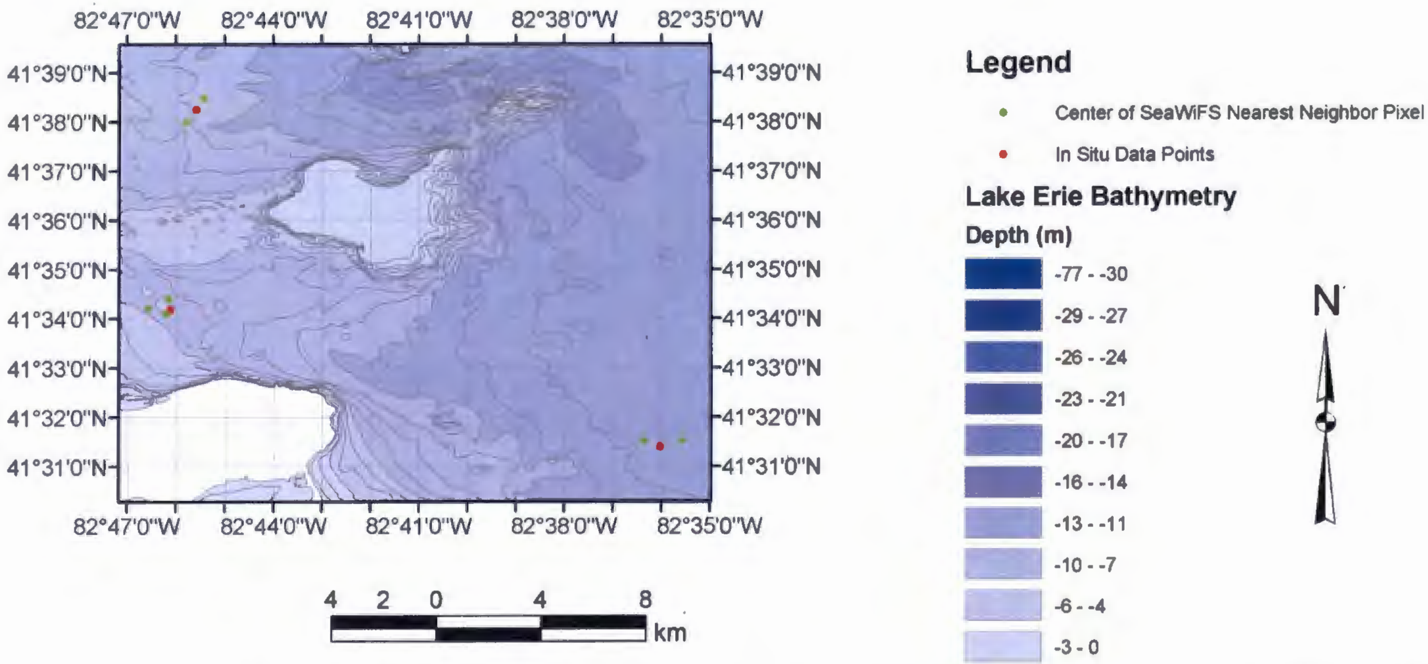

Figure 4.4: Location of the in situ data points and the SeaWiFS image pixel sample locations for the Bass Island Region of Lake Erie.

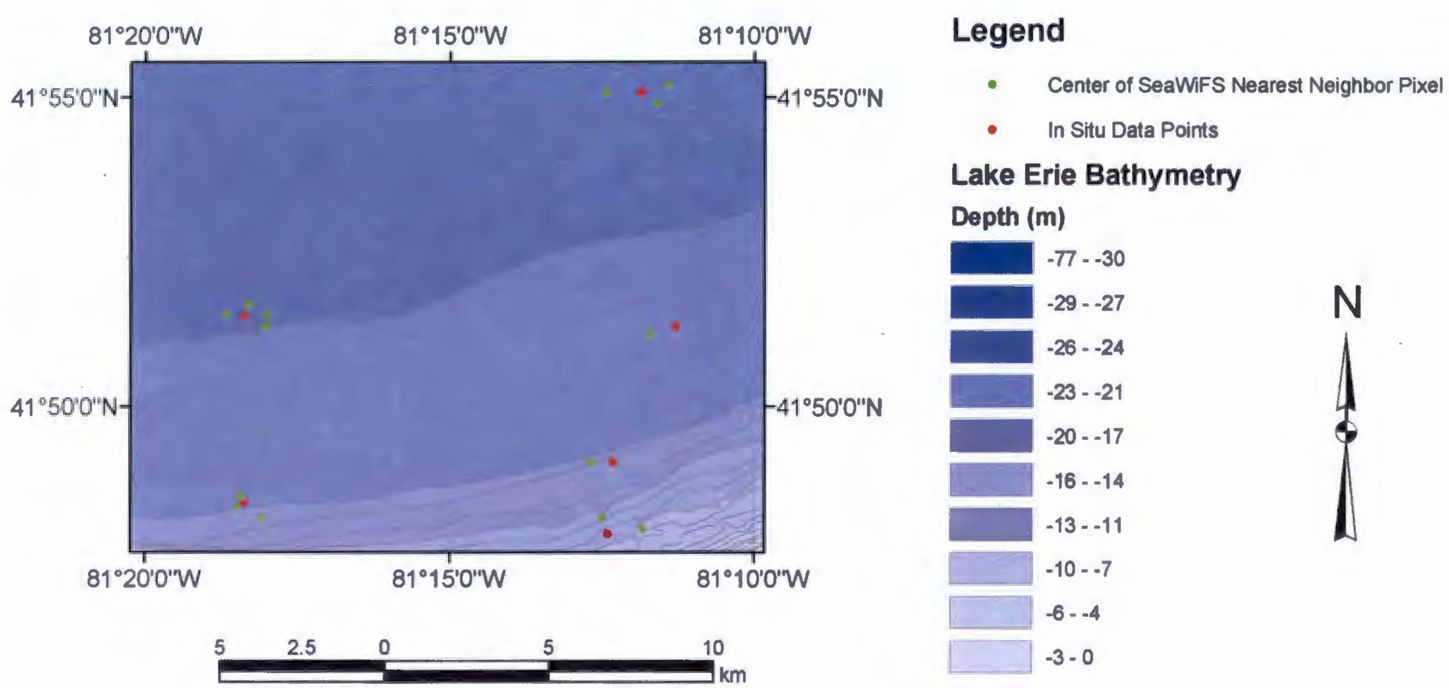

Figure 4.5: Location of the in situ data points and the SeaWiFS image pixel sample locations for the Central Basin of Lake Erie.

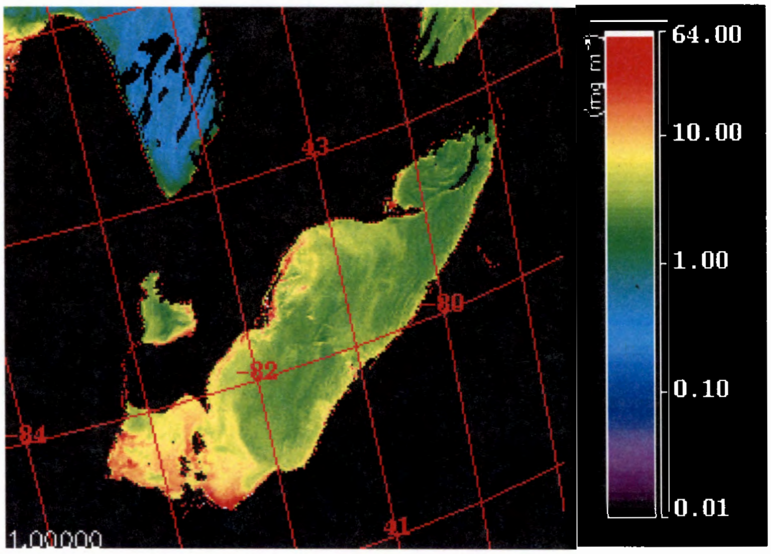

Figure 4.6: Level 2 OC4v4 image (6 September 2002) of Lake Erie generated in SeaDAS showing chlorophyll concentration (in mg/m^3).

CHAPTER 5

RESULTS

To determine the accuracy of the five ocean color algorithms and the accuracy of the sample point prediction methodology, a simple linear regression of the results of each of the algorithms and the observed chlorophyll concentration at each location was performed using the method outlined by Chatterjee and Hadi (1986). The inverse distance weighted (IDW) method was found to provide increases in R^2 values of an average of 0.11 over the nearest neighbor method (0.35 as opposed to 0.24) (Table 5.1). Of the five algorithms examined, the OC4v4 algorithm had the highest correlation (R^2 of 0.38) between observed and predicted chlorophyll concentrations.

5.1: Sampling Methodologies

Of the four sampling methodologies (nearest neighbor, bilinear averaging, spatial averaging, and inverse distance weighted), the inverse distance weighted method had the highest correlation to the observed chlorophyll values for all five ocean color algorithms. Spatial averaging was found to be the next best sampling method, followed by bilinear averaging, and then the nearest neighbor method (Table 5.1).

These results were as expected, due to the overlapping nature of the pixel data resulting from the across-track design of the SeaWiFS scanner. With each increase in spatial weight to neighboring pixels, an increase in R^2 was observed. For the nearest neighbor method, no weight is given to neighboring pixels, and the average R^2 value was found to be 0.24. The bilinear averaging method only gives weight to the adjacent four pixels, with an average R^2 value of 0.29. The spatial average method gives weight to the adjacent nine pixels and the average R^2 value was found to be 0.33. The inverse distance weighted (IDW) method gives decreasing weight to pixels located further from the in situ sample point for the entire 3x3 pixel matrix. The average R^2 value for the IDW method was found to be 0.35. As shown in Figure 5.1, the spatial variation of the constituents in the western basin of Lake Erie can be significant.

5.2: Algorithm Results

Individual algorithm and methodology results can be found in Tables 5.2-5.5. The graphs showing the predicted vs. observed chlorophyll concentrations for the five algorithms are shown in Figures 5.2 through 5.6. The dashed lines indicate a 95% confidence interval, while the solid line is the linear regression equation. All of the regressions had several points outside of the 95% confidence interval. These points occurred when the models consistently overpredicted the concentrations for three samples that were determined to have approximately 3-4 μg/L chlorophyll-a and two samples that were determined to have approximately 6 μg/L chlorophyll-a. These five samples were located in the western part of the Western basin, the easternmost point in the Bass Island region, and the northernmost point in the Central basin.

A quantile-quantile plot (Figure 5.7) of the OC4v4 algorithm results against the in situ data illustrates the differences in their distributions (Figures 4.1 and 5.8), specifically the differences in the means and standard deviations. While the in situ data has a mean of 5.24 μg/L and a standard deviation of 3.4 μg/L (Figure 4.1), the OC4v4 algorithm results had a mean of 8.01 μg/L and a standard deviation of 6.03 μg/L (Figure 5.8). This wider range of prediction using the OC4v4 algorithm results from samples where the algorithm overpredicted the chlorophyll concentration. The sample sites typically occurred at low secchi depth measurements (< 1.5 m) and shallow water depths (< 7 m). This discrepancy may result from the atmospheric correction process. In some cases, it is possible the near infrared reflection was higher than normal due to higher sediment and/or chlorophyll concentration in the surface water. The atmospheric correction algorithm uses these bands (7 and 8) to obtain "black body" values, which are then used to correct the other bands. In this case, the "black body" value obtained would be incorrect, and would result in an overcompensation for atmospheric scattering.

Figure 5.9 shows a plot of the data values used for the maximum band ratio in the OC4v4 algorithm vs. the in situ chlorophyll concentration. For comparison the OC4 (solid line) and OC4v4 (dashed line) model equations are also plotted. As shown, the fourth order polynomial equation of the OC4v4 algorithm seems to represent the observed data better than the modified cubic polynomial equation of the OC4 model.

Figure 5.10 is taken from O'Reilly et al. (2000) and is shown at the same scale as Figure 5.9. Figure 5.10 illustrates the data values used for the maximum band ratio in their development of the OC4v4 algorithm vs. the in situ chlorophyll concentration. This figure was not developed using data from Lake Erie, but from other eutrophic waters with chlorophyll concentrations similar to Lake Erie, as well as data from oligotrophic waters. When comparing Figure 5.9 with 5.10, all but one of the sample data points in Figure 5.9

is within the scatter observed for the OC4v4 algorithm. The outlying data point was taken on August 9, 2002 in the Central Basin (Figure 4.5 – the southwesternmost sample point, Table 4.1 sample point 2). This data point is abnormal not only because of the low concentration of chlorophyll (0.08 mg/L), but also because the data point is one of the highest secchi depth measurements (5.5 m). The OC4v4 algorithm predicted the chlorophyll concentration to be 2.13 μg/L. While the relative error is high for this prediction, the absolute error is 2.05 μg/L.

Figure 5.11 shows that the six highest prediction errors occurred at water depths of 6 m (the shallowest depth recorded for this data set). These sample points also corresponded to secchi depths of 1.5 m or less (Figure 5.12). Spatially, these points were located either in the western basin or closer to the shoreline (Figure 4.3 all points, Figure 4.4 southernmost two points, and Figure 4.5, southeasternmost data point). Secchi depths can be correlated to the water depth at the sample sites with an R^2 of 0.54 (Figure 5.13). This makes it difficult to determine if secchi depth or water depth or both are the major factors contributing to error in the algorithm, as absolute errors (predicted – observed values) were most significant when water depths were shallow or secchi depths were low. Secchi depth is only a measure of contrast through water and not upwelling or downwelling irradiances alone (Estep and Arnone, 1993). The bottom reflectance occurring at these shallow water depths or the scattering due to the high seston concentration indicated by low secchi depth cannot be isolated as single factors causing the errors. Chlorophyll concentrations were typically higher at low secchi depths (Figure 5.14), as well as at shallow depths (Figure 5.15). The algorithm prediction errors were also typically higher in these areas (Figures 5.11 and 5.12). This was expected due to the low secchi depth resulting from increased chlorophyll (among other constituents) concentrations and the shallow water depths, resulting in decreased light penetration. These two conditions might result in a lower band ratio being recorded by the satellite.

Overall, the OC4v4 ocean color algorithm outperformed the other four algorithms examined, however, only marginally. This was because for the sample sites examined, the 510:555 band ratio was consistently the maximum band ratio compared to the 443:555 and 490:555 band ratios, and was always used in the OC4v4 algorithm. This is important, because this ratio is the best correlated index of chlorophyll-a concentrations, when values exceed 3 mg/m^3 (O'Reilly et al., 2000). For this study 26 out of 37 sample points exceeded 3 mg/m^3. Of the algorithms examined, only the OC4v4 and OC4 algorithms were maximum band-ratio algorithms. The modified cubic polynomial form of OC4 was found to not fit the data. For the Aiken-C and Aiken-P algorithms that rely on the ratio of the water leaving radiances (L_{WN}) at 490 and 555, use of the 490:555 band ratio was found to be less important for Lake Erie. In eutrophic waters, the signal to noise ratio (SNR) increases as the wavelength value used in the numerator of the ratio increases (i.e., SNR is higher at the 510 nm wavelength than at the 412 nm wavelength) (O'Reilly et al., 2000). The CalCOFI-3 algorithm uses the 510:555 band ratio, but weighs this ratio less than the 490:555 band ratio (1.238 as opposed to 1.622). Also of note is that for the atmospheric correction scheme used in SeaDAS, "the 510 band is much less prone to extrapolation errors (resulting from a NIR atmospheric correction scheme) than the 490 nm and 443 nm bands" (O'Reilly et al., 2000). Therefore, algorithms using the 510:555 band ratio are likely to generate more accurate results.

The OC4v4 algorithm seems to be the best suited ocean color algorithm for Lake Erie. However, further refinement of this algorithm for the Lake Erie environment is warranted. As can be seen in Figure 5.9, the OC4v4 ocean color algorithm overpredicts the chlorophyll concentration for a majority of the in situ samples. Additional measurements of in situ chlorophyll concentrations are recommended to develop additional values of the 510:555 band ratio of R_{rs} to test in the OC4v4 algorithm. In this way, the coefficients shown in equation 3.6 could be refined to result in a geographic-specific ocean color algorithm for Lake Erie.

Method	Algorithm	M	b	R^2	$R^2_{average}$
Nearest Neighbor	Aiken-P	0.78	3.61	0.24	0.24
	Aiken-C	0.56	2.69	0.25	
	OC4	3.22	5.25	0.18	
	CalCOFI-3	1.44	5.07	0.25	
	OC4v4	0.99	3.03	0.30	
Bilinear averaging	Aiken-P	0.82	3.42	0.28	0.29
	Aiken-C	0.60	2.51	0.29	
	OC4	3.54	3.50	0.27	
	CalCOFI-3	1.52	4.65	0.29	
	OC4v4	0.97	2.92	0.34	
Spatial Average	Aiken-P	0.99	3.09	0.30	0.33
	Aiken-C	0.71	2.30	0.31	
	OC4	4.55	0.99	0.31	
	CalCOFI-3	1.82	3.95	0.33	
	OC4v4	1.06	2.62	0.37	
Inverse Distance Weighted	Aiken-P	0.97	2.91	0.34	0.35
	Aiken-C	0.70	2.17	0.35	
	OC4	4.22	1.19	0.33	
	CalCOFI-3	1.78	3.78	0.36	
	OC4v4	1.07	2.53	0.38	

Table 5.1: Linear regression results for the five ocean color algorithms for predicting chlorophyll concentration.

$$[Chl_{predicted}] = m \times [Chl_{observed}] + b$$

Year	Julian Day	Sample ID	In Situ	Aiken-P	Aiken-C	OC4	CalCOFI-3	OC4v4
2002	222 9 Aug	1	1.10	1.35	1.11	2.04	2.18	1.74
		2	0.08	2.12	1.27	2.58	2.74	2.11
		3	1.27	2.68	2.10	3.16	3.51	2.47
		4	0.84	5.08	3.86	6.43	7.07	4.21
	242 30 Aug	1	9.85	14.42	10.44	95.31	28.40	23.16
		2	3.85	6.37	4.79	13.69	10.18	7.13
		3	6.98	14.74	10.66	34.62	23.89	12.88
	249 6 Sep	1	8.65	11.07	8.11	25.41	17.94	10.64
		2	9.42	11.72	8.57	38.28	20.39	13.69
		3	3.69	4.78	3.64	4.80	6.23	3.40
		4	3.52	6.35	4.77	5.55	8.07	3.79
		5	4.05	3.43	2.65	3.16	4.25	2.47
		6	3.84	10.69	7.85	10.30	14.23	5.88
2003	174 23 June	1	1.61	2.18	1.29	2.60	2.80	2.12
		2	1.67	3.46	2.68	4.60	4.79	3.30
		3	3.21	1.41	1.16	2.22	2.36	1.87
		4	1.52	2.80	2.19	3.56	3.77	2.71
		5	2.42	5.67	4.29	11.20	8.87	6.22
	176 25 June	1	10.65	11.40	8.35	37.62	19.88	13.54
		2	5.42	8.91	6.60	27.69	15.43	11.23
		3	4.87	4.53	3.46	10.35	7.30	5.89
		4	5.46	2.65	2.07	4.38	3.84	3.18
	195 14 July	1	6.10	5.03	3.82	9.84	7.83	5.69
		2	15.14	14.76	10.68	50.19	25.72	16.08
		3	2.26	1.42	1.17	2.16	2.36	1.83
		4	4.15	13.64	9.90	46.72	23.85	15.41
		5	12.23	11.13	8.16	28.05	18.40	11.32
		6	9.32	6.66	4.99	16.76	11.03	8.15
		7	8.94	5.53	4.18	10.67	8.60	6.02
	210 29 July	1	3.82	24.59	17.38	115.59	44.54	25.74
		2	6.44	11.28	8.26	37.27	19.68	13.47
		3	6.08	4.58	3.49	8.33	6.98	5.07
		4	5.04	6.21	4.67	11.87	9.66	6.47
	253 10 Sep	1	3.12	1.27	1.04	2.08	2.04	1.77
	280 7 Oct	1	2.99	17.68	12.68	62.20	30.81	18.21
		2	6.35	14.05	10.19	44.00	24.13	14.88
		3	2.85	4.29	3.29	7.59	6.48	4.75

Table 5.2: Algorithm Results (μg/L) using Nearest Neighbor Sampling.

Year	Julian Day	Sample ID	In Situ	Aiken-P	Aiken-C	OC4	CalCOFI-3	OC4v4
2002	222 9 Aug	1	1.10	1.84	1.23	2.43	2.60	2.01
		2	0.08	2.25	1.48	2.88	3.03	2.30
		3	1.27	2.68	1.99	3.11	3.50	2.44
		4	0.84	4.07	3.13	5.17	5.62	3.58
	242 30 Aug	1	9.85	14.56	10.50	67.74	26.63	18.34
		2	3.85	6.01	4.53	11.90	9.41	6.47
		3	6.98	8.12	6.00	16.84	12.80	7.73
	249 6 Sep	1	8.65	9.53	7.01	22.44	15.43	9.44
		2	9.42	12.34	8.99	41.13	21.41	13.96
		3	3.69	4.06	3.12	4.12	5.26	3.03
		4	3.52	6.49	4.87	6.66	8.64	4.31
		5	4.05	4.37	3.34	4.49	5.70	3.21
		6	3.84	19.03	13.37	14.58	23.88	7.00
2003	174 23 June	1	1.61	2.07	1.29	2.71	2.85	2.19
		2	1.67	3.44	2.66	4.69	4.79	3.33
		3	3.21	1.46	1.15	2.17	2.32	1.83
		4	1.52	2.70	1.95	3.47	3.63	2.65
		5	2.42	5.42	4.10	9.77	8.25	5.57
	176 25 June	1	10.65	15.66	11.20	78.92	28.32	17.73
		2	5.42	9.78	7.19	34.47	17.12	12.08
		3	4.87	3.96	3.04	8.62	6.29	5.18
		4	5.46	2.72	2.13	4.59	3.97	3.29
	195 14 July	1	6.10	4.82	3.67	8.26	7.24	4.99
		2	15.14	19.64	13.79	77.87	33.47	16.83
		3	2.26	2.06	1.35	2.91	2.90	2.31
		4	4.15	16.08	11.57	57.58	28.11	17.18
		5	12.23	16.60	11.83	58.64	28.34	15.48
		6	9.32	7.34	5.48	18.82	12.19	8.73
		7	8.94	5.50	4.16	10.51	8.53	5.95
	210 29 July	1	3.82	20.14	14.21	104.49	36.11	20.43
		2	6.44	14.19	10.23	48.39	24.46	14.77
		3	6.08	4.56	3.48	8.37	6.96	5.08
		4	5.04	5.43	4.11	10.66	8.46	5.96
	253 10 Sep	1	3.12	1.29	1.06	2.14	2.10	1.81
	280 7 Oct	1	2.99	21.39	15.17	74.44	36.64	19.42
		2	6.35	15.01	10.84	51.65	26.09	16.06
		3	2.85	4.19	3.21	7.51	6.34	4.69

Table 5.3: Algorithm Results (μg/L) using Spatial Average Sampling.

Year	Julian Day	Sample ID	In Situ	Aiken-P	Aiken-C	OC4	CalCOFI-3	OC4v4
2002	222 9 Aug	1	1.10	1.90	1.24	2.49	2.65	2.04
		2	0.08	2.23	1.43	2.85	2.94	2.28
		3	1.27	2.65	1.97	3.12	3.47	2.45
		4	0.84	4.24	3.24	5.21	5.80	3.60
	242 30 Aug	1	9.85	13.22	9.59	69.63	24.85	18.64
		2	3.85	5.80	4.38	11.66	9.11	6.39
		3	6.98	10.55	7.71	22.77	16.79	9.55
	249 6 Sep	1	8.65	9.50	7.01	22.15	15.44	9.62
		2	9.42	12.08	8.81	38.59	20.86	13.60
		3	3.69	4.13	3.17	4.28	5.39	3.12
		4	3.52	6.28	4.72	6.34	8.31	4.16
		5	4.05	3.80	2.92	3.71	4.83	2.80
		6	3.84	11.60	8.46	10.33	15.10	5.87
2003	174 23 June	1	1.61	2.10	1.30	2.70	2.86	2.19
		2	1.67	3.56	2.75	4.81	4.96	3.39
		3	3.21	1.40	1.15	2.19	2.32	1.85
		4	1.52	2.66	1.88	3.45	3.58	2.64
		5	2.42	5.63	4.26	10.37	8.62	5.81
	176 25 June	1	10.65	15.57	11.14	69.38	27.73	16.92
		2	5.42	9.03	6.67	28.26	15.58	11.11
		3	4.87	4.06	3.12	9.02	6.49	5.35
		4	5.46	2.73	2.13	4.61	3.99	3.30
	195 14 July	1	6.10	5.42	4.11	9.64	8.26	5.61
		2	15.14	12.61	9.16	40.21	21.50	13.32
		3	2.26	1.91	1.26	2.70	2.76	2.18
		4	4.15	15.27	11.02	53.93	26.69	16.59
		5	12.23	15.11	10.83	51.95	25.74	14.52
		6	9.32	7.18	5.36	18.52	11.94	8.63
		7	8.94	5.51	4.17	10.49	8.54	5.95
	210 29 July	1	3.82	19.37	13.79	88.30	34.80	20.97
		2	6.44	12.91	9.37	42.13	22.28	14.08
		3	6.08	4.59	3.51	8.50	7.03	5.14
		4	5.04	5.92	4.47	11.85	9.29	6.43
	253 10 Sep	1	3.12	1.28	1.06	2.12	2.09	1.80
	280 7 Oct	1	2.99	20.14	14.34	64.33	34.22	18.35
		2	6.35	14.54	10.52	47.89	25.16	15.53
		3	2.85	4.22	3.23	7.66	6.41	4.76

Table 5.4: Algorithm Results (μg/L) using Bilinear Averaging Sampling.

Year	Julian Day	Sample ID	In Situ	Aiken-P	Aiken-C	OC4	CalCOFI-3	OC4v4
2002	222 9 Aug	1	1.10	1.62	1.18	2.26	2.41	1.89
		2	0.08	2.13	1.30	2.62	2.78	2.13
		3	1.27	2.70	2.05	3.15	3.53	2.47
		4	0.84	3.56	2.71	4.49	4.94	2.98
	242 30 Aug	1	9.85	12.70	9.22	69.69	24.06	18.53
		2	3.85	6.18	4.65	12.92	9.81	6.85
		3	6.98	13.86	10.03	30.72	22.16	11.72
	249 6 Sep	1	8.65	10.65	7.81	24.70	17.28	10.35
		2	9.42	11.61	8.49	37.06	20.06	13.28
		3	3.69	4.32	3.31	4.36	5.61	3.16
		4	3.52	6.15	4.63	5.91	8.01	3.96
		5	4.05	3.85	2.96	3.80	4.91	2.84
		6	3.84	15.10	10.76	12.39	19.26	6.39
2003	174 23 June	1	1.61	2.19	1.31	2.69	2.87	2.18
		2	1.67	3.48	2.69	4.64	4.82	3.32
		3	3.21	1.47	1.16	2.18	2.34	1.84
		4	1.52	2.71	1.95	3.43	3.62	2.63
		5	2.42	4.46	3.36	8.58	6.92	4.70
	176 25 June	1	10.65	12.99	9.42	50.26	22.93	15.00
		2	5.42	8.87	6.56	27.77	15.33	11.07
		3	4.87	4.45	3.40	10.10	7.16	5.79
		4	5.46	2.68	2.10	4.49	3.90	3.23
	195 14 July	1	6.10	5.05	3.84	9.06	7.69	5.36
		2	15.14	19.47	13.73	78.56	33.65	17.95
		3	2.26	1.96	1.31	2.73	2.79	2.19
		4	4.15	14.38	10.41	50.65	25.18	16.01
		5	12.23	15.06	10.80	49.67	25.52	14.33
		6	9.32	6.78	5.08	16.77	11.18	8.12
		7	8.94	5.53	4.19	10.68	8.60	6.03
	210 29 July	1	3.82	20.23	14.36	94.91	36.43	21.51
		2	6.44	15.46	11.12	54.12	26.86	16.20
		3	6.08	4.58	3.50	8.39	7.00	5.09
		4	5.04	6.06	4.57	11.64	9.43	6.38
	253 10 Sep	1	3.12	1.28	1.05	2.11	2.08	1.80
	280 7 Oct	1	2.99	18.54	13.26	64.65	32.14	18.48
		2	6.35	15.12	10.92	51.18	26.24	16.11
		3	2.85	4.20	3.22	7.49	6.35	4.69

Table 5.5: Algorithm Results (μg/L) using IDW Sampling

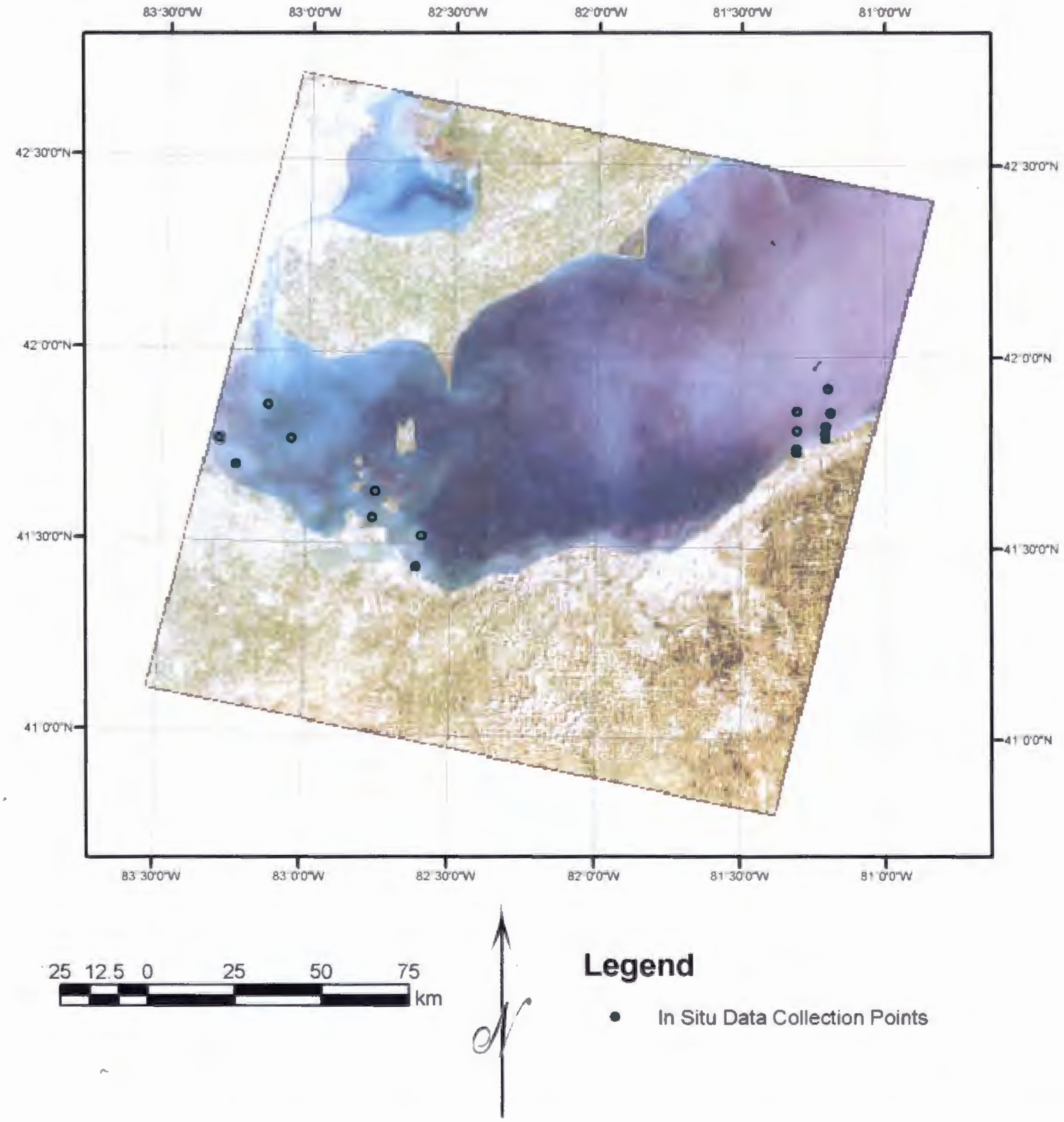

Figure 5.1: Landsat-7 image of Western and Central Basins of Lake Erie for August 1, 2002. The locations of the 2002 and 2003 sampling points used in this analysis are also plotted.

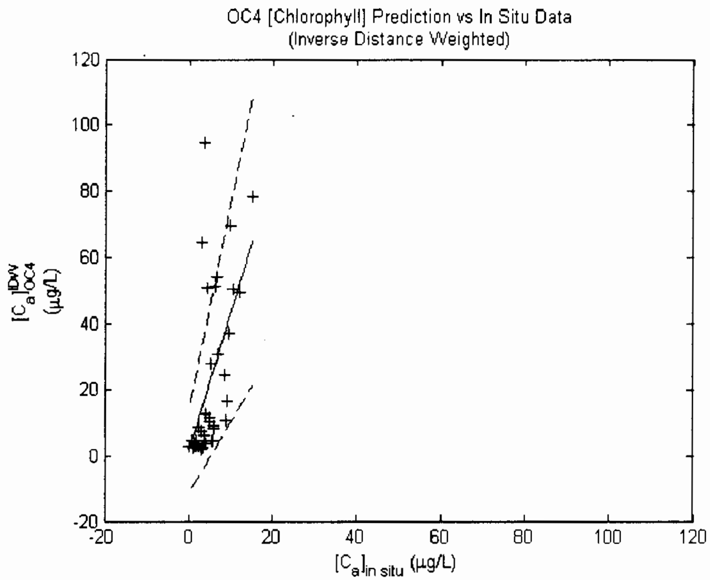

Figure 5.2: OC4 Prediction (IDW) vs In Situ Data.

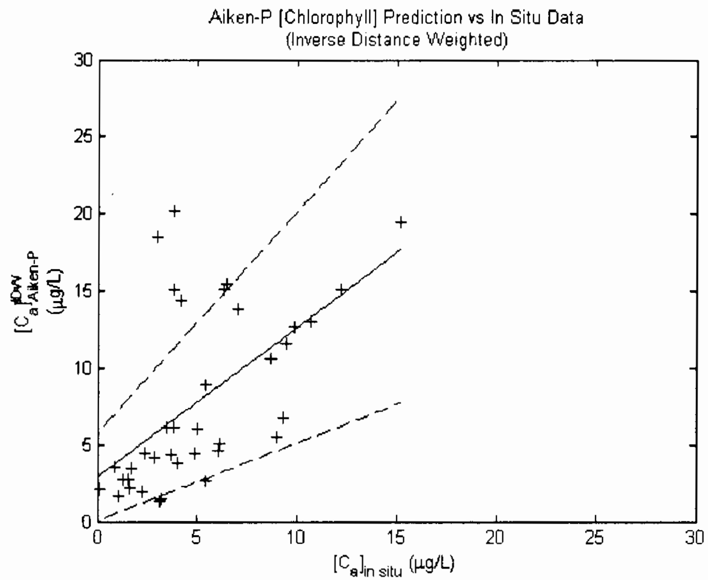

Figure 5.3: Aiken-P Prediction (IDW) vs In Situ Data.

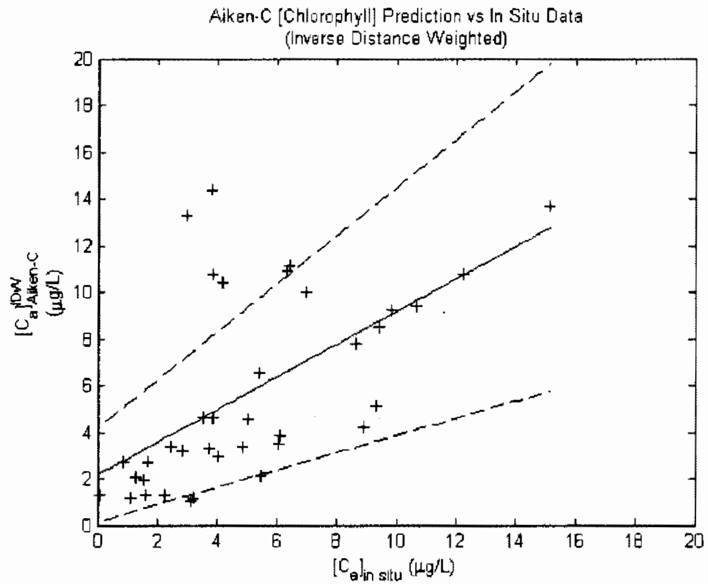

Figure 5.4: Aiken-C Prediction (IDW) vs In Situ Data.

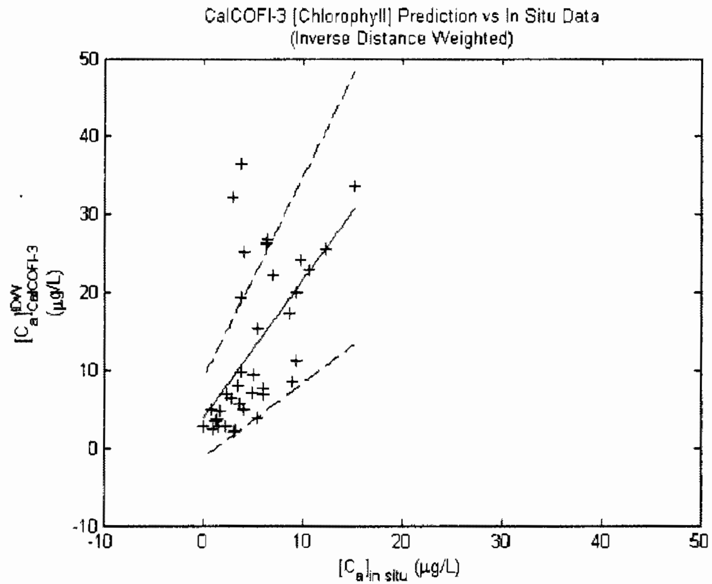

Figure 5.5: CalCOFI-3 Prediction (IDW) vs In Situ Data.

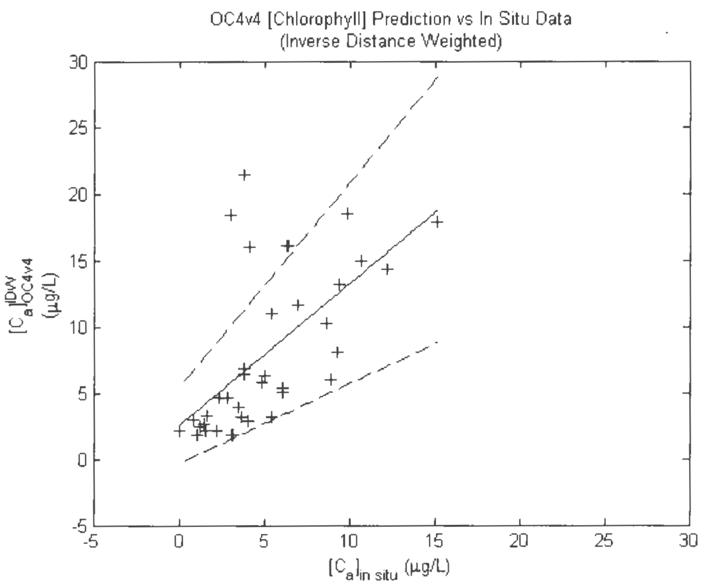

Figure 5.6: OC4v4 Prediction (IDW) vs In Situ Data.

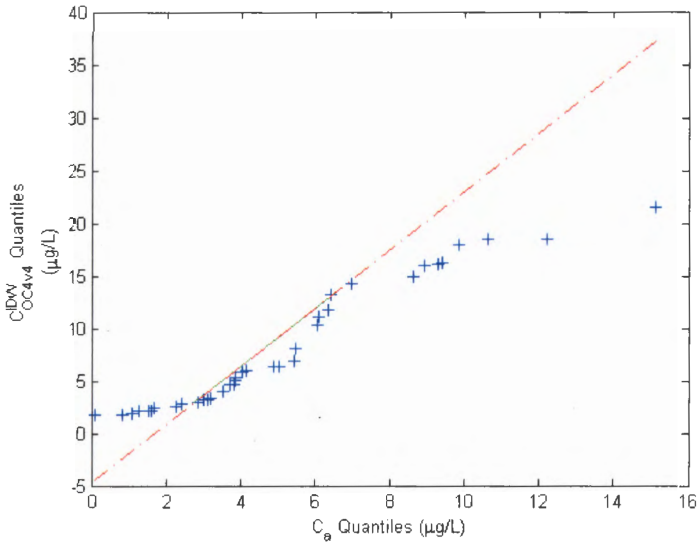

Figure 5.7: Quantile-quantile plot of OC4v4 Prediction (IDW) versus In Situ Data.

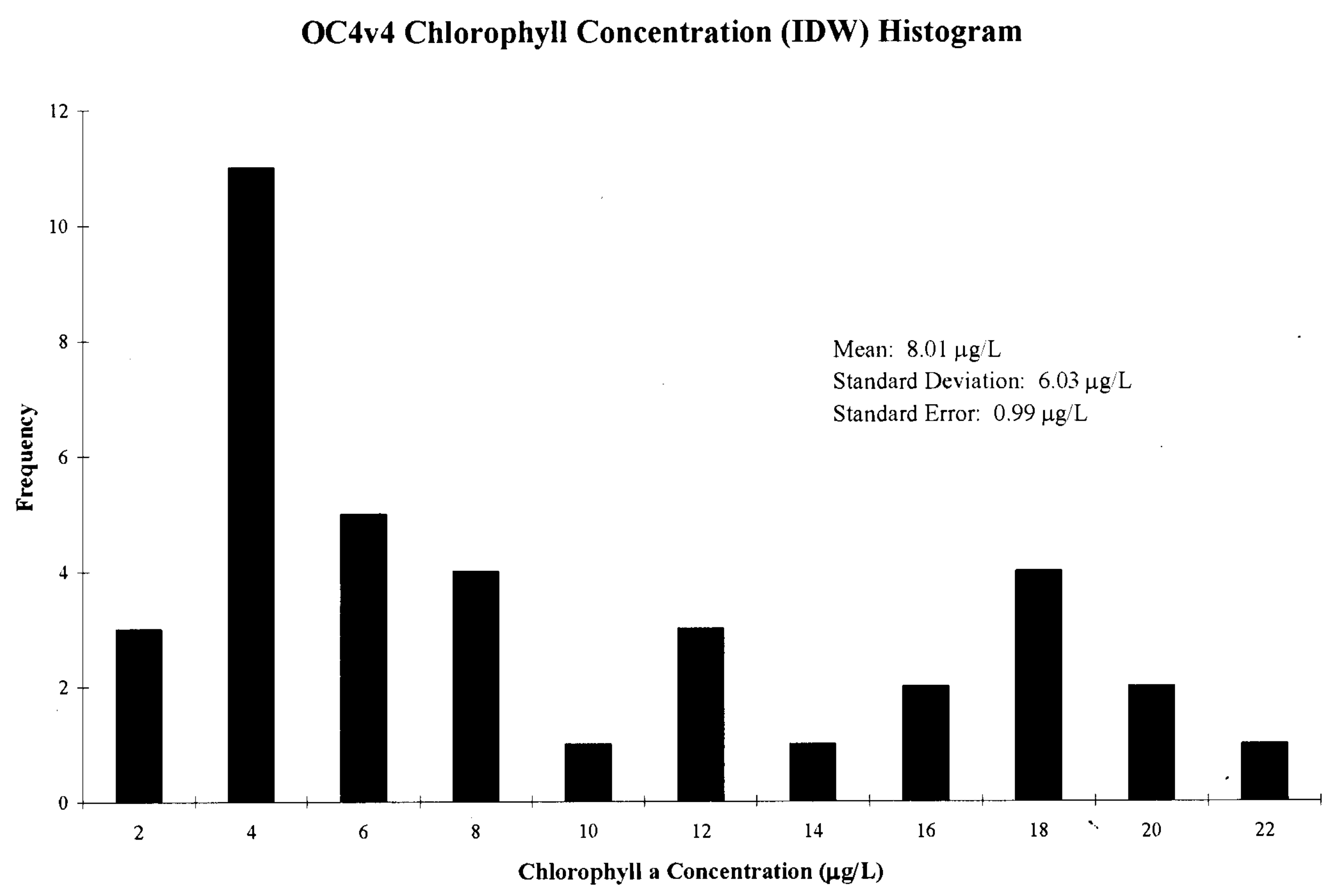

Figure 5.8: Histogram of OC4v4 (IDW) Chlorophyll Concentrations.

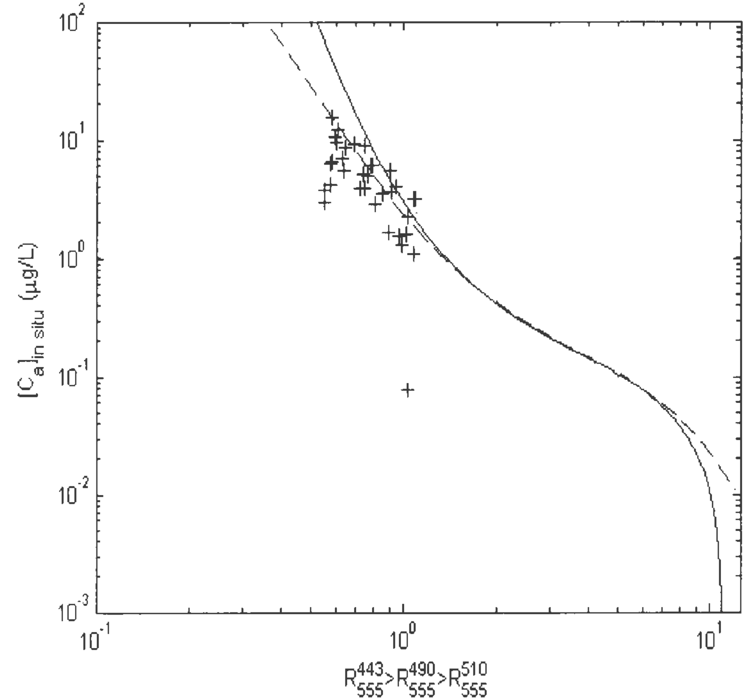

Figure 5.9: Maximum R vs In Situ Chlorophyll. Also shown is the OC4 model (solid curve) and OC4v4 model (dashed curve).

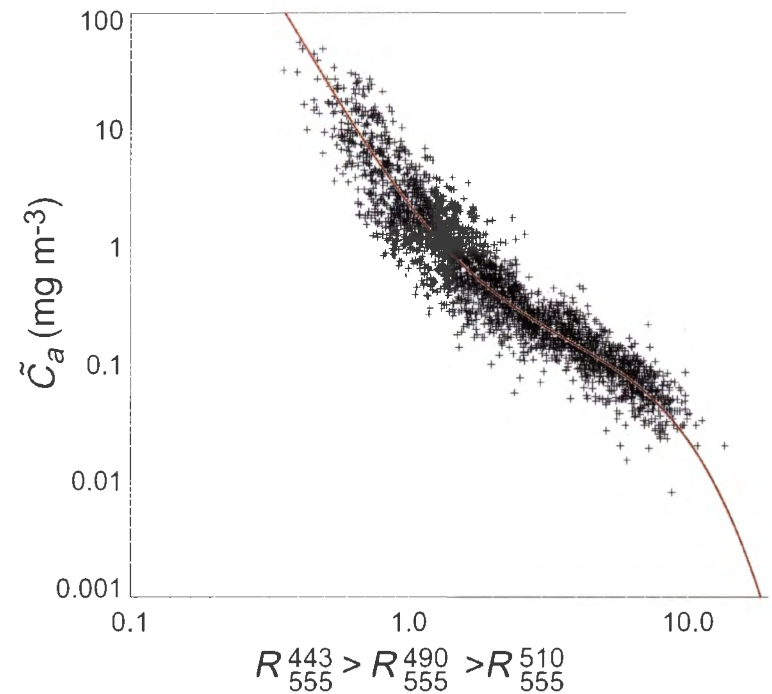

Figure 5.10: Maximum R vs In Situ Chlorophyll for 2,853 in situ ocean color observations. Also shown is the OC4v4 model (solid curve) [from O'Reilly et al. 2000].

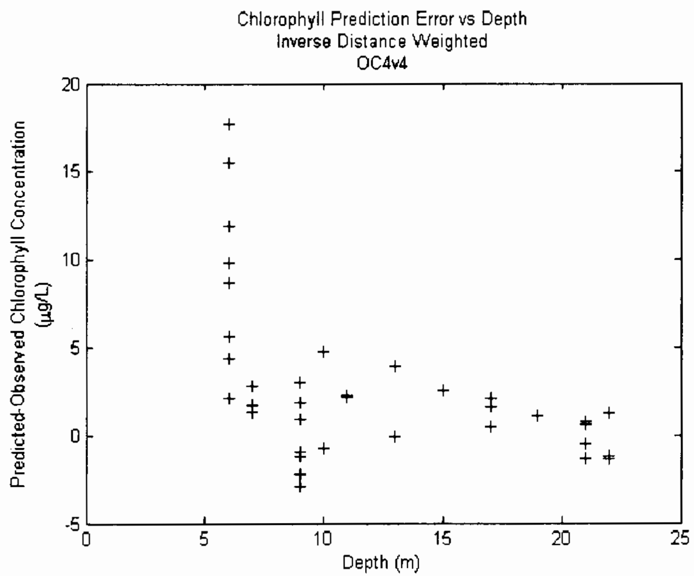

Figure 5.11. OC4v4 Prediction Error vs Depth (IDW).

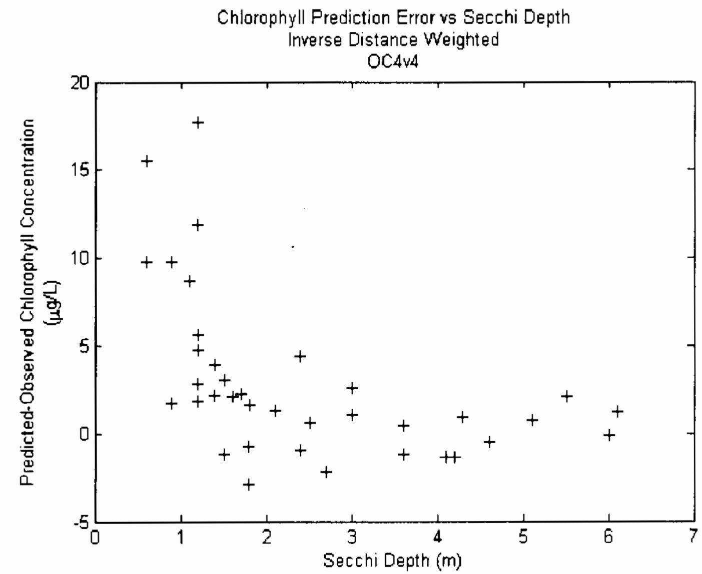

Figure 5.12: OC4v4 Prediction Error vs Secchi Depth.

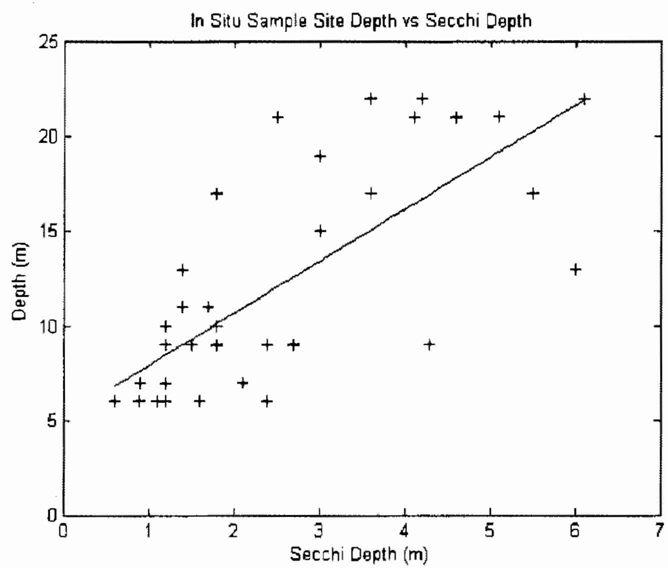

Figure 5.13: In Situ Sample Site Depth vs Secchi Depth – R^2=0.54.

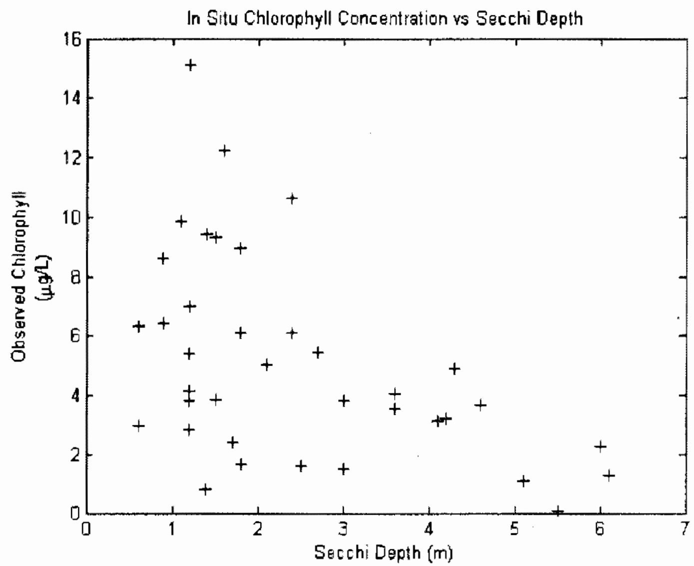

Figure 5.14: In Situ Chlorophyll Concentration vs Secchi Depth.

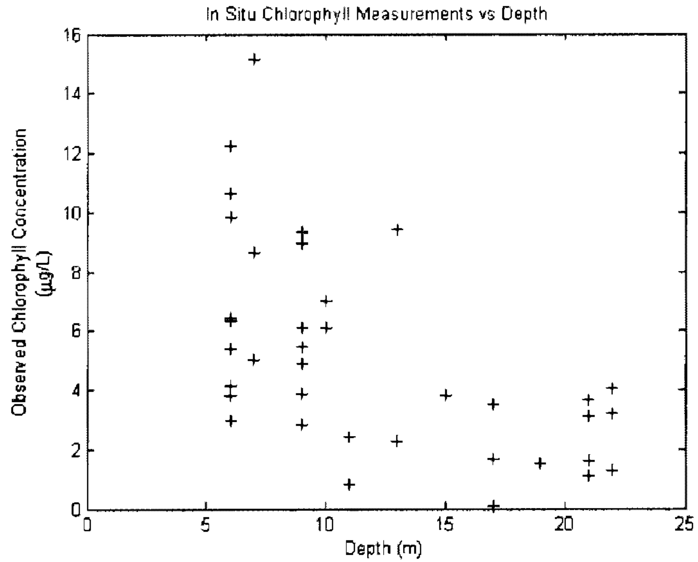

Figure 5.15: In Situ Chlorophyll Measurements vs Water Depth.

CHAPTER 6
DISCUSSION

To investigate the significance of the R^2 values obtained in the linear regressions performed, the t test was examined. The student t test determines whether the observed sample correlations are significantly different from zero. If the two variables are independent, then the R values occurred because of randomness. For a sample of 37 pairs of measurements (35 degrees of freedom) and a 95% level of significance, the critical value for t is ~1.69. For the OC4v4 method, the t statistic was found to be 4.63. Because the test statistic falls into the upper critical region, the correlation between the in situ data and the predicted chlorophyll concentrations is statistically significant. The results of the t test for the five algorithms can be found in Table 6.1.

Method	$t_{observed}$	Significant at 95% level
Aiken-P	4.25	Yes
Aiken-C	4.34	Yes
CalCOFI-3	4.44	Yes
OC4	4.15	Yes
OC4v4	4.63	Yes

Table 6.1: Results of student t test for the IDW method for the algorithms examined.

The results from this t test imply that the predicted chlorophyll concentrations for all of the models are indeed related to the in situ chlorophyll concentrations observed. This implies that differences in both the normalized water leaving radiances and remotely sensed reflectances are, at least in part, due to differences in chlorophyll concentrations. The R^2 values of approximately 0.35 indicate that only 35% of the variability in the predictions can be accounted for by the remote sensing measurements. Also, the correlations observed in this studywere lower than those found for the studies used in the development of the algorithms.

When predicted chlorophyll concentrations were plotted vs. the observed chlorophyll for all five algorithms (Figures 5.2 through 5.6), using the t test method outlined by Zar (1984), no statistical differences were found in either the slopes ($\alpha(2)$ = 0.05, DF = 70, t = 0.25, P = 0.71) or the intercepts ($\alpha(2)$ = 0.05, DF = 70, t = 0.11, P = 0.78) between the OC4v4 and Aiken-P models (Table 6.2). The Aiken-P and Aiken-C algorithms were found to also have no statistical differences in the intercepts ($\alpha(2)$ = 0.05, DF = 70, t = -1.85, P = 0.07), however, their slopes differed.

Algorithms	OC4v4 vs. Aiken-P		Aiken-P vs. Aiken-C
Property	Slopes	Intercepts	Intercepts
$\alpha(2)$	0.05	0.05	0.05
Degrees of Freedom	70	70	70
t	0.25	0.11	-1.85
P	0.71	0.78	0.07

Table 6.2. Results of regression analysis for the IDW method for relationships found to be significant

This implies that the two Aiken models tend to overpredict chlorophyll consistently, however, there is a base constant difference (2.91 - 2.17 = 0.74 μg/L), between their overprediction. The Aiken-P and OC4v4 algorithms might have the same slope and intercept values, indicating that the prediction results are similar. The higher R^2 value of the OC4v4 algorithm (0.38 as opposed to 0.34 – Table 5.1) indicates that the algorithm results are influenced slightly more (4%) by changes in the optical properties of the water, resulting from changes in the chlorophyll concentrations than in the Aiken-P algorithm. Statistical differences were found in the slopes and intercepts between all other models, since the relationships failed t tests.

The current goal of the SeaWiFS project is to be able to predict chlorophyll to within ±35% in open ocean water (Hooker et al., 1992). However, this standard when applied to Case II watersmay not be achievable. Work by Hu et al. (1998) in the North-Central Gulf of Mexico showed that at low concentrations (~0.7 mg/L), even modified chlorophyll algorithms, specifically designed to account for turbidity, experience errors as high as 655%. Hu et al. (1998) indicated that in shallow water (<10 m) where chlorophyll concentrations are low, the bottom reflected light contributes to the measured remote sensing reflectance. This is not likely in the case of the western and central basins of Lake Erie examined for this study, as secchi depth was never greater than half the water depth, making suspended sediment a more likely factor in the measured remote sensing reflectance than bottom reflectance. A linear regression of secchi depth against predicted chlorophyll concentration (Figure 6.1) illustrates the relationship. The t test for this linear regression (α=0.05, DF=35, t_{crit}=1.69, t=5.43) signifies that the correlation is significantly different than zero. The R^2 value from the linear regression implies that

46% of the variability in the model is due to constituents in the water column. The secchi depth gives us a relative measure of the depth where these constituents occur. This is 8% more than the effects of chlorophyll (R^2=0.46 from Figure 6.1 as opposed to R^2=0.38 from Table 5.1), although chlorophyll most likely has a direct effect on the secchi depth. This implies that at least 16% (1 - 0.46 - 0.38 = 16%) of the variability in the model cannot be explained by secchi depth or chlorophyll concentrations. This remaining error most likely results from the atmospheric correction scheme used in the SeaDAS software.

The guidelines for chlorophyll detection established by Stumpf (1987) for AVHRR imagery are within 60% for concentrations greater than 10 μg/L and within 5 μg/L at concentrations below 10 μg/L. Using these guidelines, three of the algorithms (Aiken-C, Aiken-P, and OC4v4) on average performed within the margin of error. For concentrations greater than 10 μg/L, the Aiken-P algorithm overpredicted thechlorophyll concentration on average by 25%, while the Aiken-C algorithm predicted below the measured concentration on average by 11% (Table 6.2). The OC4v4 algorithm averaged 26% overprediction of chlorophyll. However, there were only three in situ data where chlorophyll was greater than 10 μg/L, making these findings inconclusive. For concentrations less than 10 μg/L (which comprised 34 of the 37 data points), the Aiken-P algorithm averaged 2.73 μg/L overpediction, the Aiken-C algorithm averaged 0.81 μg/L overprediction, and the OC4v4 algorithm averaged 2.90 mg/L overprediction. CalCOFI-3 did not meet either of the guidelines, averaging 7.15 μg/L over prediction for chlorophyll concentrations less than 10 μg/L, and an average of 115% overprediction for chlorophyll concentrations greater than 10 μg/L. The OC4 algorithm did not meet either of these guidelines.

The standard deviations of the absolute errors were 4.71 μg/L for the Aiken-P algorithm, 3.48 μg/L for the Aiken-C algorithm, and 4.75 μg/L for the OC4v4 algorithm. These standard deviations were slightly less than the 5 μg/L guidelines. For the OC4 and CalCOFI-3 algorithms, the standard deviations of the absolute errors were 23.63 μg/L and 8.73 μg/L, respectively. These standard deviations exceeded the 5 μg/L guidelines.

Algorithm	[C] > 10 μg/L % Error	[C] < 10 mg/L Error (μg/L)	Standard Deviation of Absolute Errors (μg/L)
Aiken-P	25%	2.74	4.71
Aiken-C	-11%	0.81	3.48
OC4	366%	15.04	23.63
CalCOFI-3	115%	7.15	8.73
OC4v4	26%	2.90	4.75

Table 6.3. Prediction Errors for the IDW method for the algorithms examined.

Work by Mupparthy and Merry (2004) experienced similar complications, wherein all five models typically underpredicted the in situ concentration measurements (Table 6.3).

Table 6.4. Prediction Error and Standard Deviation of Prediction Error from Mupparthy and Merry (2004).

Model	Average Prediction Error (μg/L)	Standard Deviation of Error (μg/L)
OC4	-22.5	25.7
OC4v4	-2.1	68.7
Aiken-P	-1.7	36.0
Aiken-C	-2.3	33.7

CalCOFI-3	-14.6	3.5

Mupparthy and Merry (2004) also examined in situ optical data and compared these data with the satellite-derived estimates. They found that their prediction errors principally resulted from errors in the atmospheric correction algorithm. The errors in the optical data "clearly indicate that atmospheric correction is still a big issue when dealing with lake systems like Lake Erie." The in situ chlorophyll concentrations examined by Mupparthy and Merry (2004) were on the same order of magnitude as this study (~9.2 ± 10.6 μg/L in their study compared to 5.1 ± 3.4 μg/L for this study). Atthe higher concentrations examined (27 μg/L) the models evaluated in their studyunderestimated the chlorophyll concentration by between 24 and 91%, while at lower concentrations (2-4 μg/L) "most of the algorithms overestimate the concentrations."

Harding et al. (1995) also encountered prediction errors when developing an algorithm for the Chesapeake Bay using aerial remote sensing methods. Using a spectroradiometer with three bands: R_1=460 nm, R_2=490 nm, and R_3=520 nm, Harding et al. (1995) developed an algorithm using the following form:

$$\log 10[Chl] = a + b\left(\log 10\left(\frac{R_2^2}{R_1 R_3}\right)\right) \tag{6.1}$$

Where a and b were empirically-derived constants. When the predicted chlorophyll concentrations were compared to the measured chlorophyll concentrations, R^2 values ranged from 0.30-0.40. After binning (grouping) the data at 0.005 mg/L intervals, the R^2 values increased to 0.63-0.82. They found that at low chlorophyll concentrations (~2 mg/L), their results tended to be accurate. However, at high chlorophyll concentrations (>10 mg/L) their algorithm results overestimated the in situ measurements by 200-400%.

Clearly the models examined are reflecting changes in optical propertiesof the water due to increases in chlorophyll concentrations. However, other constituents in the Case II waters of Lake Erie are interfering with a direct calculation of chlorophyll concentration. Carder et al. (1991) found that substances, such as colored dissolved organic matter (CDOM) in Case II waters, can cause calculated chlorophyll pigment concentrations to have inaccuracies as high as 133%. Constituents affecting secchi depth, as well as possibly bottom reflectance, have been shown to affect the atmospheric correction scheme used. This will then resultin miscalculation of Rayleigh scattering in the atmosphere, directly affecting the results of the algorithms. A measurement of total suspended solids (TSS) or turbidity data for the data set in this study would be necessary to understand the reflectance measurements being measured by the SeaWiFS instrument.

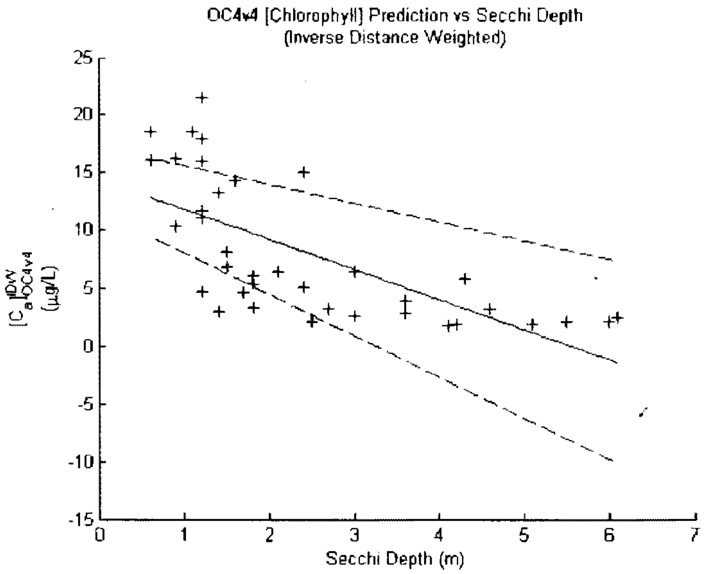

Figure 6.1. Oc4v4 Prediction (IDW) vs Secchi Depth with 95% confidence interval (R^2=0.46).

CHAPTER 7
CONCLUSIONS

Four methods to determine a representative satellite pixel value to be used in the ocean color algorithm calculations were examined. The method of inverse distance weighted (IDW) interpolation provided a slight benefit to the end results. The IDW method showed an increase in reliability (0.10 increase in R^2) of prediction for all five algorithms.

Of the five ocean color algorithms evaluated, the OC4v4 algorithm was found to provide the best prediction for the western and central basins of Lake Erie. The OC4v4 algorithm had the highest coefficient of determination (R^2=0.38) between predicted and in situ chlorophyll concentrations. The CalCOFI-3 algorithm was found to be nearly as good (R^2=0.36), with the Aiken-C algorithm (R^2=0.35) ranking third. If more in situ data were available for statistical verification, an algorithm similar in form to the Ocean Chlorophyll fourth-order polynomial four-band algorithm (OC4v4) may be best suited for the Lake Erie area, since this algorithm seemed to perform best in this study. The accuracy of the model OC4v4 declined, as the water depth decreased below 7 m and the secchi depth decreased to 1.5 m. This may severely hinder monitoring of cyanobacteria, such as *Microcystis*, for drinking water intake purposes, since many of the water intakes are located in waters less than 15 m deep – where secchi depths are typically shallow.

CHAPTER 8
FUTURE WORK

Chlorophyll concentration mapping from satellite imagery of the Great Lakes, and in particular Lake Erie, is problematic due to the dynamic spatial variations of constituents. Influences from bottom reflectance, suspended sediments, and other suspended materials have effects on the ocean color algorithms examined. The atmospheric correction scheme used is also critical in determining the water reflectance characteristics.

On May 4, 2002, the AQUA satellite was launched with the Moderate Resolution Imaging Spectroradiometer (MODIS) onboard. MODIS has 36 spectral bands and is a 12-bit radiometric sensor with a 250-1000 m spatial resolution (depending upon the band) and a daily temporal resolution. "MODIS is typically 2-3 times more [radiometrically] sensitive than SeaWiFS" (Gordon and Voss, 1999) and the bands are one-half to one-fourth as wide as SeaWiFS, with comparable spectral coverages (Figure 7.1) (SeaWiFS bands 7 and 8 are 765 ± 20 nm and 865 765 ± 20 nm, respectively, while MODIS bands 15 and 16 are 750 ± 5 nm and 865 ± 7 nm, respectively). With the additional sensitivity and spectral bands more alternatives exist for determining band ratio correlations and for developing better atmospheric correction schemes.

Carder et al. (2003) evaluated the viability of the MODIS sensor in determining chlorophyll-a concentrations in Case II waters. They suggested that there be three classifications of regions of chlorophyll concentrations – packaged, transitional, and unpackaged – based on the difference between the sea surface temperature and the nitrate depletion temperature. This was previously not possible due to the lack of a thermal sensor onboard the SeaStar satellite. This is because the difference "provides a means of estimating how packaged were the pigments for a given pixel" (Carder et al., 2003). Packaged pigments are low ratios of photoprotective pigments to chlorophyll and high self-shading. Unpackaged pigments are "high ratios of photoprotective pigments to chlorophyll and low self-shading." (Carder et al., 2003). Transitional pigments are a global-average type. Preliminary results of this method produced results accurate to about 30% (Carder et al., 2003) for the SeaWiFS Bio-optical Algorithm Mini-Workshop (SeaBAM) dataset.

While the algorithm examined by Carder et al. (2003) does not take into account the turbidity of the water directly, their method does take into account an absorption coefficient for phytoplankton, gelbstoff, and the diffuse attenuation coefficient, which can be related to secchi depth. Future work on MODIS or SeaWiFS data should examine turbidity and total suspended solids (TSS) data, as well as optical profiles. These measurements would provide more information on interference from bottom reflectance and scattering due to TSS, suspended sediment, chlorophyll or other optical constituents. The additional channels in MODIS also provide more information to use in atmospheric correction algorithms used over lake and ocean waters (bands 24, 25, and 27-36) (Menzel et al., 2002).

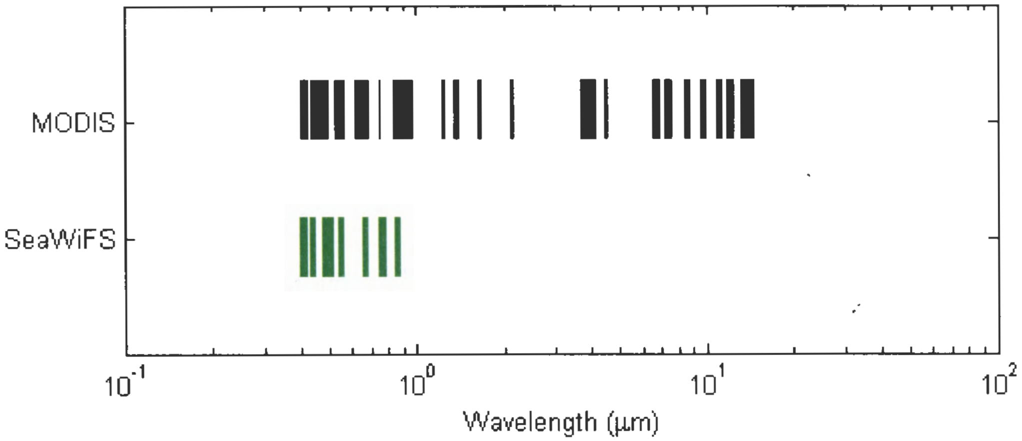

Figure 8.1. Spectral band coverage of the MODIS and SeaWiFS sensors.

LITERATURE CITED

Acker, J., 1994. The Heritage of SeaWiFS: A Retrospective on the CZCS NIMBUS Experiment Team (NET) Program [S. Hooker and E. Firestone eds.], *SeaWiFS Technical Report Series 21,* NASA Goddard Space Flight Center, Greenbelt, MD.

Aiken, J., Moore, G., Trees, C., Hooker, S., and Clark, D., 1995. The SeaWiFS CZCS-Type Pigment Algorithm [S. Hooker and E. Firestone eds], *SeaWiFS Technical Report Series 29,* NASA Goddard Space Flight Center, Greenbelt, MD

Arar, E., 1997. In Vitro Determination of Chlorophylls a, b, c1+c2 and Pheopigments in Marine and Freshwater Algae by Visible Spectrophotometry, *Methods for the Determination of Chemical Substances in Marine and Estuarine Environmental Matrices – 2nd Edition,* National Exposure Research Laboratory, Office of Research and Development, U.S. Environmental Protection Agency, Cincinnati, Ohio. Method 446, 26pp.

Bisset, W., Schofield, O., Cullen, J., Plueddemann, A., and Mobley, C., 2001. Resolving the Impacts and Feedback of Ocean Optics on Upper Ocean Ecology, *Oceanography,* 14(3), 30-53

Budd, J., Beeton, A., Stumpf, R., Culver, D., and Keerfoot, W., 2001. Satellite Observations of Microcystis blooms in western Lake Erie, *Proceedings of the International Association of Theoretical and Applied Limnology,* Dublin, August 9-24, 1998, 2787-3793

Carder, K.L., S.K. Hawes, K.A. Baker, R.C. Smith, R.G. Steward, and B.G. Mitchell, 1991. Reflectance model for quantifying chlorophyll a in the presence of productivity degradation products, J. Geophys. Res., 96, 20,599–20,611

Carder, K.L., Chen, F.R., Lee, Z., Hawes, S.K., and Cannizzaro, J.P., 2003. MODIS Ocean Science Team Algorithm Theoretical Basis Document, ATBD 19 "Case 2 Chlorophyll a". Version 7, 30 January, College of Marine Science, University of South Florida.

Chandler, L., 1998. SeaWiFS completes a year of remarkable earth observations. *Press Release 98-170.* Goddard Space Flight Center, Greenbelt, MD. 17 September 1998.

Chatterjee, S. and A. S. Hadi, 1986. Influential Observations, High Leverage Points, and Outliers in Linear Regression. Statistical Science, pp. 379- 416.

Culver, D., Baker, D., Richards, R., Beeton, A., Johengen, T., Leshkevich, G., Vanderploeg, H., Budd, J., Carmichael, W., Heath, R., Wickstrom, C., MacIsaac, H., and Wu, L., 1999. Toxicity, ecological impact, monitoring, causes, and public awareness of Microcystis blooms in Lake Erie. Final Report to the Lake Erie Commission. Ohio State University, Columbus, OH.

Environment Canada and United States Environmental Protection Agency (USEPA), 1995. Great Lakes Atlas.

Environment Canada and United States Environmental Protection Agency (USEPA), 2003. State of the Great Lakes 2003.

ESRI, 2003. Deterministic methods for spatial interpolation *ArcGIS 9: Using ArcGIS Geostatistical Analyst*, 113-131.

Estep, L., and Arnone, R. 1993. Correlation of CZCS Surface K's with K's Derived from Secchi Disk. Proceedings, First Thematic Conference on Remote Sensing for Marine and Coastal Environments, New Orleans, LA, June 15-17, 1992. American Society for Photogrammetry and Remote Sensing, 459-471

Fujiki, H., Sueoka, E., and Suganuma, M., 1996. Carcinogenesis of Microcystins. *Toxic Microcystis*, [M. Watanabe, K. Harada, W. Carmichael, H Fujiki, eds.], CRC Press, Inc.: Boca Raton, Florida, 203-232

Gordon, H. and Morel, A., 1983. *Remote Assessment of Ocean Color for Interpretation of Satellite Visible Imagery, A Review*, Springer-Verlag, New York, NY

Gordon, H., and Voss, K., 1999. MODIS Normalized Water-leaving Radiance Algorithm Theoretical Basis Document (MOD 18) Version 4. Department of Physics, University of Miami. 30 April 1999

Harding, L., Itsweire, E., and Esaias, W. 1995. Algorithm development for recovering chlorophyll concentrations in the Chesapeake Bay using aircraft remote sensing, 1989-91. Photogramm. Eng. Rem. Sens. 61: 177-185

Hooker, S., Esaias, W., Feldman, G., Gregg, W., and McClain, C., 1992. An Overview of SeaWiFS: and Ocean Color [S. Hooker and E. Firestone eds], *SeaWiFS Technical Report Series 1,* NASA Goddard Space Flight Center, Greenbelt, MD

Hu, C., K. L. Carder, and F. Müller-Karger, 1998. Preliminary algorithm to derive chlorophyll pigment concentration and DOM absorption in turbid coastal waters from SeaWiFS imagery. PORSEC Quingdao, China, Proceedings, 1998. 888-892

Kuiper-Goodman, T., Falconer, I., and Fitzgerald, J., 1999. Human Health Aspects. *Toxic Cyanobacteria in Water* [I. Chorus and J. Bartram eds.], Spon Press., London, 113-153

Leahy, S., 2003. An Erie Decline. *World Press Review.* August, 2003. 50(8)

Lillesand, T., Kiefer, R., and Chipman, J., 2004. *Remote Sensing and Image Interpretation, Fifth Edition.* John Wiley & Sons, Inc. New York, NY

Menzel, W., Seemann, S., Li, J., and Gumley, L., 2002. MODIS Atmospheric Profile Retrieval Algorithm Theoretical Basis Document Version 6. University of Wisconsin-Madison, 10 October 2002

Mitchell, B., and Kahru, M., 1998. Algorithms for SeaWiFS Standard Products Developed with the CalCOFI Bio-Optical Data Set, *CalCOFI Rep.* 39, Calif. Coop. Oceanic Fish. Invest. Rep., Lajolla, Calif., 26 pp.

Mupparthy, R., and Merry, C., 2004. Analysis of Ocean Color Algorithms for Lake Erie. *Proceedings of ASPRS Conference*, Denver, Colorado, CD-ROM, May 23-28, 2004, 14p.

NASA Earth Observatory, 2002. "Overview of the Earth Science Enterprise". 29 May 2002. Internet Source, http://earthobservatory.nasa.gov/Library/ESE/ese.html

NASA Procurement Office, 2005. Notice of Intent to Award on a Sole Source Basis, Solicitation Number: NNS05092321, http://prod.nais.nasa.gov/cgi-bin/eps/synopsis.cgi?acqid=114262

NOAA Sea Grant, 1995. Thick Slick of Green Ick: Bloom of Blue-Green Algae Returns to Lake Erie, *Sea Grant News Release,* 26 October 1995.

O'Reilly, J.E., S. Maritorena, B.G. Mitchell, D.A. Siegel, K.L. Carder, S.A. Garver, M. Kahru, and C. McClain. 1988. Ocean color chlorophyll algorithms for SeaWiFS. J. Geophysical Research 103(C11): 24,937-24,953.

O'Reilly, J., Maritorena, S., Siegel, D., O'Brien, M., Toole, D., Mitchell, B., Kahru, M., Chavez, F., Strutton, P., Cota, G., Hooker, S., McClain, C., Carder, K., Muller-Karger, F., Harding, L., Magnuson, A., Phinney, D., Moore, G., Aiken, J., Arrigo, K., Letelier, R., and Culver, M., 2000. Ocean Color Chlorophyll A Algorithms for SeaWiFS, OC2, and OC4: Version 4. [S. Hooker and E. Firestone eds.], *SeaWiFS Postlaunch Technical Report Series, (11) SeaWiFS postlaunch calibration and validation analyses: part 3,* NASA Goddard Space Flight Center, Greenbelt, MD, 9-23

Park, H., and M. Watanabe, 1996. Toxic Microcystis in Eutrophic Lakes. *Toxic Microcystis*, [M. Watanabe, K. Harada, W. Carmichael, H Fujiki, eds.], CRC Press, Inc.: Boca Raton, Flrida, 57-77

Ruddick, K., Ovidio, F., and Rijkeboer, M., 2000. Atmospheric Correction of SeaWiFS imagery for turbid coastal and inland waters", *Applied Optics*, 39, pp 897-912.

SeaDAS Development Group, 2002. "l1agen command". 8 August 2002. Internet Source, http://seadas.gsfc.nasa.gov/doc/l1agen/l1agen.html

Siegel, D., Wang, M., Maritorena, S., and Robinson, W., 2000. Atmospheric correction of satellite ocean color imagery:. the black pixel assumption", *Applied Optics*, 39., pp 582-3591.

Sivonen, K., and Jones, G., 1999. Cyanobacterial Toxins. *Toxic Cyanobacteria in Water* [eds. I. Chorus, J. Bartram], Spon Press.: London, 41-111

Stumpf, R., 1987. *Application of AVHRR satellite data to the study of sediment and chlorophyll in turbid coastal water*, NOAA Technical Memorandum·NESDIS AISC 7, Washington, DC.

Zar, J., 1984. Comparing Simple Linear Regression Equations. Biostatistical Analysis. pp. 292-299

Zilberg, B. 1966. Gastroenteritis in Salisbury European children – a five-year study. *Cent. Afr. J. Med.*, 12(9), 164-168

APPENDIX A

Figure A.1: Quasi-true-color composite of SeaWiFS level 1A bands 6, 5, and 1 for August 9, 2002

Figure A.2: Quasi-true-color composite of SeaWiFS level 1A bands 6, 5, and 1 for August 30, 2002

Figure A.3: Quasi-true-color composite of SeaWiFS level 1A bands 6, 5, and 1 for September 6, 2002

Figure A.4: Quasi-true-color composite of SeaWiFS level 1A bands 6, 5, and 1 for June 23, 2003

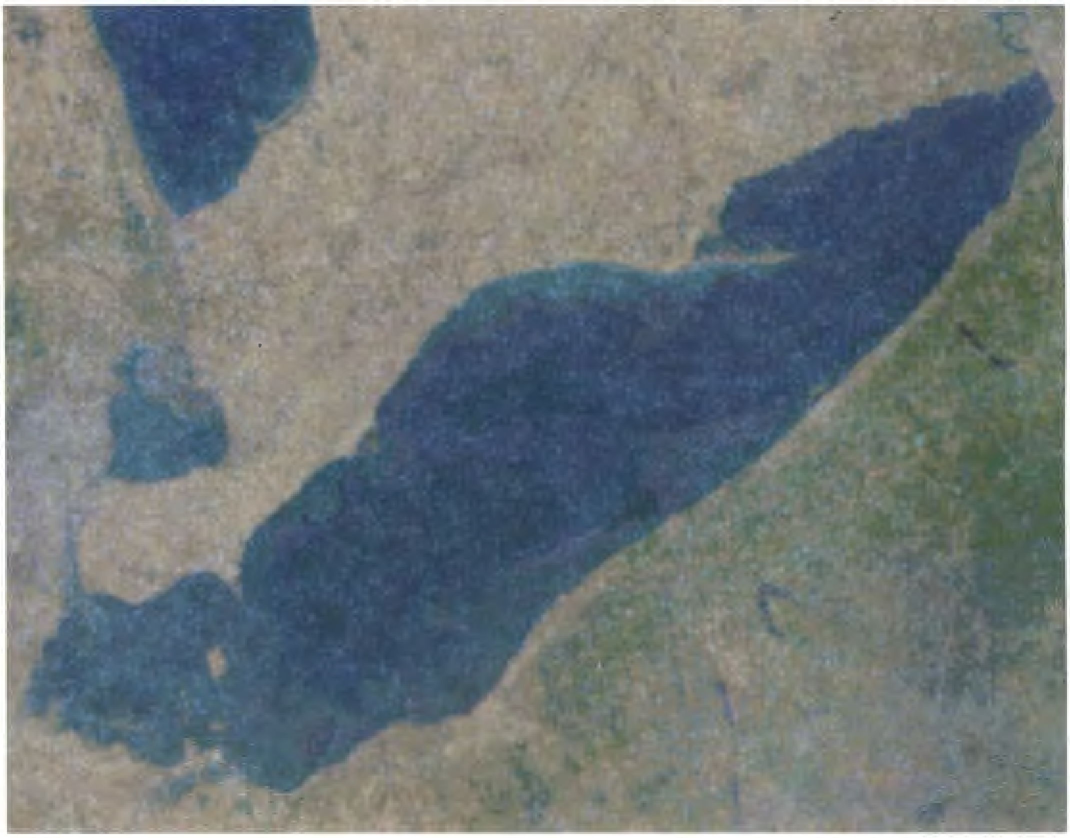

Figure A.5: Quasi-true-color composite of SeaWiFS level 1A bands 6, 5, and 1 for June 25, 2003

Figure A.6: Quasi-true-color composite of SeaWiFS level 1A bands 6, 5, and 1 for July 14, 2003

Figure A.7: Quasi-true-color composite of SeaWiFS level 1A bands 6, 5, and 1 for July 29, 2003

Figure A.8: Quasi-true-color composite of SeaWiFS level 1A bands 6, 5, and 1 for September 10, 2003

Figure A.9: Quasi-true-color composite of SeaWiFS level 1A bands 6, 5, and 1 for October 7, 2003